

# A LOCALLY-CONSERVATIVE PROXIMAL GALERKIN METHOD FOR POINTWISE BOUND CONSTRAINTS

GUOSHENG FU<sup>1</sup>, BRENDAN KEITH<sup>2</sup>, AND RAMI MASRI<sup>2</sup>

**ABSTRACT.** We introduce the first-order system proximal Galerkin (FOSPG) method, a locally mass-conserving, hybridizable finite element method for solving heterogeneous anisotropic diffusion and obstacle problems. Like other proximal Galerkin methods, FOSPG finds solutions by solving a recursive sequence of smooth, discretized, nonlinear subproblems. We establish the well-posedness and convergence of these nonlinear subproblems along with stability and error estimates under low regularity assumptions for the linearized equations obtained by solving each subproblem using Newton’s method. The FOSPG method exhibits several advantages, including high-order accuracy, discrete maximum principle or bound-preserving discrete solutions, and local mass conservation. It also achieves prescribed solution accuracy within asymptotically mesh-independent numbers of subproblems and linear solves per subproblem iteration. Numerical experiments on benchmarks for anisotropic diffusion and obstacle problems confirm these attributes. Furthermore, an open-source implementation of the method is provided to facilitate broader adoption and reproducibility.

*Key words.* Anisotropic diffusion, obstacle problems, high order accuracy, local mass conservation, discrete maximum principle preserving

*MSC codes.* 35J86, 49J40, 65N30.

## 1. INTRODUCTION

We propose the first-order system proximal Galerkin (FOSPG) method for second-order, elliptic energy principles with pointwise bound constraints. The method, given below in Algorithm 2, is based on the proximal Galerkin method proposed in [46] and features (i) high-order accuracy, (ii) bound preservation at every point in the computational domain (not only at nodal/quadrature points), and (iii) local mass conservation. To the best of our knowledge, this is the first finite element method with these three properties.

We choose to focus our presentation on two categories of model problems: heterogeneous anisotropic diffusion and (unilateral/bilateral) obstacle problems. These two types of model problems have a multitude of applications, with the first appearing in reservoir simulations [1] and plasma physics [35]. The second is vital for optimal control [58], topology optimization [55], and glaciology [37], among many other applications. Although much remains to be learned, we have found that FOSPG is highly accurate and efficient for solving these two categories of problems and so aim to promote its use in scientific applications involving them.

---

<sup>1</sup> DEPARTMENT OF APPLIED AND COMPUTATIONAL MATHEMATICS AND STATISTICS (ACMS), UNIVERSITY OF NOTRE DAME, NOTRE DAME, IN 46556

<sup>2</sup> DIVISION OF APPLIED MATHEMATICS, BROWN UNIVERSITY, PROVIDENCE, RI 02912

*E-mail addresses:* gfu@nd.edu, brendan.keith@brown.edu and rami\_masri@brown.edu.

*Date:* December 31, 2024.

GF was supported in part by NSF DMS-2410740. BK and RM were supported in part by the U.S. Department of Energy Office of Science, Early Career Research Program under Award Number DE-SC0024335.

**1.1. Heterogeneous anisotropic diffusion.** The exact solutions of certain boundary value problems satisfy pointwise bound constraints almost everywhere in the domain. This property is known as the weak maximum principle [48]. A long-sought feature of numerical approximations is to satisfy this maximum principle while maintaining high-order accuracy.

Fundamental links have been established between discrete maximum principle (DMP) preserving first-order finite element methods and local mesh properties. This connection has been known since the seminal work of Ciarlet [21], which identifies the non-obtuse angle condition as a key condition ensuring DMP preservation for *isotropic* diffusion. Several relaxations of this condition have been established subsequently. For example, [63] shows that Delaunay meshes with obtuse angles near diffusion discontinuities also preserve the DMP.

DMP-preserving local mesh conditions are more delicate to derive and difficult to enforce for anisotropic diffusion. In particular, weakly acute angle conditions formulated with respect to the diffusion tensor need to be enforced on the internal dihedral angles of the mesh [52]. However, generating such anisotropy-aligned meshes can be very challenging or infeasible [35, 36]. Recently, *nonlinear* schemes satisfying the DMP without any mesh restrictions have been proposed [18, 10, 2, 8]. However, these schemes typically have low-order accuracy or enforce DMP only at nodal points [18, 8]. It is also unclear whether these approaches can preserve mass locally. We refer readers to the recent review article [9] for a more detailed account of DMP-preserving finite element methods and further references.

**Unique properties:** FOSPG is DMP-preserving at every point in the computational domain, regardless of the polynomial degree employed. Moreover, the method is locally mass-conservative and does not require anisotropy-aligned meshes.

**1.2. Obstacle problems.** Minimizing a quadratic energy functional over a closed, non-empty, convex set results in a variational *inequality* [20, Section 6.9]. We refer to [48] for a comprehensive introduction. The obstacle problem, modeling the equilibrium position of an elastic membrane lying above an obstacle, is the prototypical example in this problem class. Here, we present a brief overview of the standard finite element approaches to solving the obstacle problem; see [46, Section 3], [44], and [39] for additional details.

The most well-known and widely-used approach is the quadratic penalty method, which relaxes the bound-constrained optimization problem into an unconstrained one by adding terms to the energy functional that grow quadratically with the violation of the constraint [60, 53]. However, to maintain the accuracy of high-order finite elements, the penalty parameter needs to scale suitably with the mesh size and polynomial degree, leading to mesh-dependent ill-conditioning [39]. Alternatively, one can discretize the variational inequality directly using the primal formulation [16] or the mixed formulation [15]. However, the low regularity of the Lagrange multiplier associated with the inequality constraint in these formulations affects the performance of numerical solution techniques [42], often making penalty methods more desirable [43, 3]; see also [30, Section 4.1]. A different mixed formulation is also obtained by introducing a Lagrange multiplier, modeling the contact pressure [38, 62]. For this formulation to be inf-sup stable, one enriches the finite element spaces with bubble functions or uses consistent stability terms [39]. The latter option leads to another penalty method for piecewise linear elements or to a Nitsche-type penalty method when broken polynomial spaces are used for the multiplier [39]. We refer to [38] for analyzing the latter class of methods.

Techniques from nonlinear programming are often employed to solve discretized variational inequalities. Unfortunately, naive “first-discretize-then-optimize” approaches typically lead to

mesh-dependence; i.e., the number of nonlinear solves required for convergence grows indefinitely with mesh refinement [41, 42, 46]. Of the most prominent techniques, we highlight the primal-dual active set (or semi-smooth Newton) method [41] and the augmented Lagrangian method [33]. We also wish to highlight that multigrid methods often help accelerate convergence and diminish mesh-dependence [17]; we refer to [34] for a detailed overview.

It is well-known that one can enforce pointwise bound constraints, such as pointwise non-negativity, by constraining the nodal values of linear elements [16]. However, enforcing pointwise constraints on higher order approximations is far more difficult [49]. We refer to [46, Section 3.2] for an overview. Proximal Galerkin methods overcome this challenge by constructing discrete solutions in the image of a bound-preserving monotone map. The resulting algorithm consists of solving a sequence of smooth, semilinear PDE systems that couple standard finite element variables to a so-called latent variable in the domain of the nonlinear map [46]. Analogs of this algorithm have been extended to density-based topology optimization [45, 47] and a multitude of other challenging problems such as elastic contact, variational fracture, gradient constraints, and obstacle-type quasi-variational inequalities [23]. Efficient preconditioners and  $hp$ -adaptive schemes for proximal Galerkin have also been proposed in [54], exhibiting  $hp$ -robustness in the number of Newton linear solves and up to 20x speed-ups over state-of-the-art methods. In this work, we show that the essential features of the proximal Galerkin method are maintained for mass-conserving discretizations.

**Unique properties:** FOSPG has a low iteration complexity and does not require mesh-dependent penalty parameters. It also provides a discrete solution that satisfies prescribed bound constraints at every point in the computational domain and achieves high-order accuracy. Further, it delivers a locally-conservative flux approximation in every element not intersecting the obstacle contact zone.

**1.3. Main contributions and outline.** The outline of this paper and its main contributions are summarized below.

- In Section 2, we state the anisotropic diffusion and obstacle problems that motivate this work. Here, we demonstrate that the former problem can be formulated as a variational inequality, a property allowing us to unify our exposition.
- We review the latent variable proximal point (LVPP) algorithm in Section 3. We then derive the first-order system proximal Galerkin (FOSPG) method from this algorithm; cf. Algorithm 2. We then prove the existence and uniqueness of solutions to the FOSPG subproblems and their stability properties in Theorem 4.2 and Lemma 4.3.
- In Section 4.3, we present a hybridized form of the FOSPG method, given in Algorithm 3. We advocate for this approach because, after static condensation, the linearized FOSPG subproblems in Algorithm 3 reduce to sparse, symmetric positive definite systems involving only the mesh facet unknowns. This convex structure is particularly convenient for applying Newton's method to solve the subproblems. Algorithm 3 is used in the practical implementation of our method.
- In the main theoretical result, Theorem 5.3, we prove convergence of Algorithms 2 and 3 to the solution  $u_h^*$  of a discrete variational inequality for simplicial elements with polynomial degree  $p = 0$  and quadrilateral elements for any  $p \geq 0$ . We then prove that FOSPG is locally mass-conserving on all elements where  $u_h^*$  does not come in contact with the obstacle or bound constraint. For  $p = 0$ , error estimates between the exact solution and the iterates of Algorithm 3 are also established.

- Section 6 contains stability and convergence analysis of the linearized subproblems that result from applying Newton’s method to every (nonlinear) proximal subproblem in FOSPG. This analysis is carried out for the hybridized method in Algorithm 3 and is valid for any polynomial degree  $p \geq 0$  on simplicial and quadrilateral meshes. Notably, this section focuses on low-regular solutions in order to remain valid for heterogeneous anisotropic diffusion.
- Finally, the performance of our method and its key features (high order accuracy, local mass conservation, and mesh independence) are demonstrated on a series of numerical examples in Section 7. We share our implementation, <https://github.com/ramimasri/FOSPG-first-order-system-proximal-Galerkin.git>, in NGSolve [59] to facilitate broader adoption and reproducibility.

**1.4. Notation.** In what follows,  $\Omega$  is an open bounded Lipschitz domain in  $\mathbb{R}^d$ . We use standard notation for the Lebesgue spaces  $L^p(\Omega)$  for  $p \in [1, \infty]$  and for the Sobolev–Hilbert spaces  $H^m(\Omega)$  for  $m \in \mathbb{N}$ . The space  $H^{1/2}(\partial\Omega)$  is the standard trace space of  $H^1(\Omega)$ . For  $g \in H^{1/2}(\partial\Omega)$ , the space  $H_g^1(\Omega)$  is the closed subspace of  $H^1(\Omega)$  consisting of functions  $u$  with trace  $\text{tr}(u) = g$  on  $\partial\Omega$ . Further, we use the notation  $(\cdot, \cdot)$  to denote the  $L^2(\Omega)$ -inner product. The spaces  $W^{s,p}(\Omega)$  ( $s \geq 0, p \in [1, \infty]$ ) denote the standard Sobolev spaces. We follow the convention that  $0 \ln 0 = 0$  and define the essential domain of a proper function  $f: \mathbb{R}^d \rightarrow \mathbb{R} \cup \{+\infty\}$  as

$$\text{dom } f := \{x \in \mathbb{R}^d \mid f(x) < \infty\}.$$

We consider a conforming partition  $\mathcal{T}_h$  of  $\Omega$  into elements  $T$ . Denote by  $\mathcal{E}_h$  the set of facets  $E$  (edges in 2D/ faces in 3D) of the partition  $\mathcal{T}_h$ , and denote by  $\partial\mathcal{T}_h$  the set of all element boundaries  $\partial T$  with outward normal  $\mathbf{n}$ . We assume that each element  $T$  and facet  $E$  are generated by an affine map  $\Phi_T$  or  $\Phi_E$  from a reference element  $\hat{T}$  or  $\hat{E}$ , respectively. For quadrilateral elements, this assumption means that we only consider parallelograms in 2D and parallelotopes in 3D. Although this assumption can be relaxed in practical implementations. The diameters of an element  $T$  and of a facet  $E$  are denoted by  $h_T$  and  $h_E$  respectively. The mesh size is given by  $h = \max_{T \in \mathcal{T}_h} h_T$ . For constants  $W$  and  $Q$ , we use the notation  $W \lesssim Q$  whenever there is a constant  $C$  independent of the mesh size  $h$  such that  $W \leq CQ$ . For a symmetric positive definite matrix  $A$ , we define  $A^{1/2}$  as the matrix satisfying  $A^{1/2}A^{1/2} = A$ .

The space  $H^1(\mathcal{T}_h)$  denotes the broken  $H^1$  space corresponding to the mesh  $\mathcal{T}_h$ :

$$H^1(\mathcal{T}_h) = \{u \in L^2(\Omega) : u|_T \in H^1(T), \forall T \in \mathcal{T}_h\}.$$

The broken gradient is denoted by  $\nabla_h$ , meaning that  $(\nabla_h v)|_T = \nabla(v|_T)$  for  $v \in H^1(\mathcal{T}_h)$ . We also use the broken divergence operator,  $(\nabla_h \cdot v)|_T = \nabla \cdot (v|_T)$ . Further, for all  $q, \varphi \in L^2(\partial\mathcal{T}_h)$  and  $v, w \in L^2(\Omega)$ , we use the notation

$$(q, \varphi)_{\partial\mathcal{T}_h} = \sum_{T \in \mathcal{T}_h} \int_{\partial T} q\varphi \, ds, \quad (v, w)_{\mathcal{T}_h} = \sum_{T \in \mathcal{T}_h} \int_T vw \, dx.$$

## 2. MODEL PROBLEMS

We have introduced FOSPG to target the two model problems given below. As we demonstrate, Problem 1 can be seen as a specific version of Problem 2. However, these two problems usually have different mathematical assumptions affecting their analyses.

**Problem 1** (Heterogeneous anisotropic diffusion). *Consider the following model problem:*

$$(1a) \quad -\nabla \cdot (A\nabla u) = f \quad \text{in } \Omega,$$

$$(1b) \quad u = g \quad \text{on } \partial\Omega.$$

Here,  $A \in L^\infty(\Omega; \mathbb{R}^{d,d})$  is a symmetric diffusion tensor with eigenvalues that are uniformly lower and upper bounded by positive constants,  $f \in L^2(\Omega)$  and  $g \in H^{1/2}(\partial\Omega)$ . The Lax–Milgram Theorem [28, Section 25.2] provides the existence and uniqueness of the weak solution  $u \in H_g^1(\Omega)$  to (1) satisfying

$$(2) \quad (A\nabla u, \nabla v) = (f, v) \quad \forall v \in H_0^1(\Omega).$$

**Problem 2** (Obstacle problem). *Solve for  $u \in K \cap H_g^1(\Omega)$  such that*

$$(3a) \quad J(u) \leq J(v) \quad \forall v \in K \cap H_g^1(\Omega), \quad J(v) = \frac{1}{2}(A\nabla v, \nabla v) - (f, v),$$

where the closed and convex set  $K$  is given by

$$(3b) \quad K = \{u \in H^1(\Omega) \mid \underline{u} \leq u \leq \bar{u} \text{ a.e. in } \Omega\}.$$

Here,  $\underline{u}, \bar{u} \in L^\infty(\Omega)$  and the above problem is called the bilateral obstacle problem. We also allow  $\bar{u} = \infty$  to include the unilateral obstacle problem. To ensure that  $K$  is nonempty, we assume that  $\underline{u} \leq g \leq \bar{u}$  a.e. on  $\partial\Omega$ . The existence and uniqueness of solutions follow from [48, Theorem 2.1]. Further, the above problem is equivalent to a variational inequality over  $K \cap H_g^1(\Omega)$ , see [19, Theorem 1.1.2]: Solve for  $u \in K \cap H_g^1(\Omega)$  such that

$$(4) \quad (A\nabla u, \nabla(v - u)) \geq (f, v - u) \quad \forall v \in K \cap H_g^1(\Omega).$$

We now demonstrate that Problem 1 can be equivalently formulated in the setting of Problem 2 with constant  $\underline{u}$  and  $\bar{u}$ . Indeed, if  $f \in L^q(\Omega)$  for  $q > d$ , the weak solution  $u \in H_g^1(\Omega)$  of (1) satisfies the weak maximum principle [48, Theorem 5.5 and Theorem B.2]

$$(5) \quad \|u\|_{L^\infty(\Omega)} \leq \|f\|_{L^q(\Omega)} + \sup_{\mathbf{x} \in \partial\Omega} |g|.$$

Further, if  $f \geq 0$  a.e. in  $\Omega$ , then we can also ensure that  $u \geq \inf_{\mathbf{x} \in \partial\Omega} g$  a.e. in  $\Omega$  [48, Theorem 5.7]. That is, there exist constants  $\underline{u}$  and  $\bar{u}$  such that the weak solution  $u$  belongs to the set  $K \cap H_g^1(\Omega)$ . In addition,  $u$  solves (4) since  $v - u \in H_0^1(\Omega)$  for any  $v \in K \cap H_g^1(\Omega)$  and since  $u$  satisfies (2). By uniqueness of solutions,  $u$  is both the solution to (4) and to (3a).

In practice, the diffusion tensor in Problem 1 can have very low regularity. Yet, the fact that the exact solution satisfies a variational equation can simplify error estimates, cf. Theorem 5.4 and [49, Theorem 1]. On the other hand, the diffusion tensor in Problem 2 usually has higher regularity when the obstacles  $\underline{u}, \bar{u}: \Omega \rightarrow \mathbb{R} \cup \{-\infty\} \cup \{+\infty\}$  are non-trivial functions. However, in this case, we cannot depart from the variational inequality (4).

### 3. THE LATENT VARIABLE PROXIMAL POINT ALGORITHM

The Latent Variable Proximal Point (LVPP) algorithm (see Algorithm 1) was introduced in [46] to derive numerical methods for solving variational inequalities like (4). A first-order system finite element discretization of this algorithm leads to the FOSPG method. Here, we present a derivation of LVPP based in part on the exposition in [23].

---

**Algorithm 1** The Latent Variable Proximal Point Algorithm
 

---

- 1: **input:** Initial latent solution guess  $\psi^0 \in L^\infty(\Omega)$ , a sequence of positive step sizes  $\{\alpha^k\}$ , and a Carathéodory function  $\Upsilon: \Omega \times \mathbb{R} \rightarrow \mathbb{R}$ , where  $\Upsilon(x, \cdot)$  is an increasing bijection from  $\mathbb{R} \rightarrow (\underline{u}(x), \bar{u}(x))$  for a.e.  $x \in \Omega$ .
  - 2: Initialize  $k = 1$ .
  - 3: **repeat**
  - 4: Solve the following (nonlinear) saddle-point problem: Find  $u \in H_g^1(\Omega)$  and  $\psi \in L^\infty(\Omega)$  such that
 
$$(6a) \quad \alpha^k (A \nabla u, \nabla v) + (\psi, v) = \alpha^k (f, v) + (\psi^{k-1}, v) \quad \forall v \in H_0^1(\Omega),$$

$$(6b) \quad (u, \varphi) - (\mathcal{U}(\psi), \varphi) = 0 \quad \forall \varphi \in L^\infty(\Omega),$$
 where  $\mathcal{U}(\psi)(x) := \Upsilon(x, \psi(x))$  for a.e.  $x \in \Omega$ .
  - 5: Assign  $\psi^k \leftarrow \psi$  and  $k \leftarrow k + 1$ .
  - 6: **until** a convergence test is satisfied.
- 

**3.1. Superposition operators.** Algorithm 1 relies on a Carathéodory function  $\Upsilon: \Omega \times \mathbb{R} \rightarrow \mathbb{R}$ , whose restrictions  $\Upsilon(x, \cdot)$  are monotonically-increasing, invertible functions taking  $\mathbb{R}$  to  $(\underline{u}(x), \bar{u}(x))$ . For any sufficiently regular map  $\psi: \Omega \rightarrow \mathbb{R}$ , one can then generate a new function  $\mathcal{U}(\psi): \Omega \rightarrow \mathbb{R}$  via the expression  $\mathcal{U}(\psi)(x) = \Upsilon(x, \psi(x))$ . The resulting operator  $\mathcal{U}$  is called a superposition (Nemytskii) operator [5, 4]. In Section 4, we will see that these operators allow us to construct approximate solutions to the minimization problem (3) that are guaranteed to respect pointwise bound constraints.

One can select among different choices for the generating function  $\Upsilon$ . The following two examples are appropriate for double obstacle and anisotropic diffusion problems:

$$(7a) \quad \text{Example 1:} \quad \Upsilon(x, z) = \frac{\underline{u}(x) + \bar{u}(x) \exp z}{1 + \exp z};$$

$$(7b) \quad \text{Example 2:} \quad \Upsilon(x, z) = \frac{1}{2}(\underline{u}(x) + \bar{u}(x)) + \frac{1}{2}(\bar{u}(x) - \underline{u}(x)) \frac{z}{\sqrt{1 + z^2}}.$$

Meanwhile, for the unilateral obstacle problem ( $\bar{u} = \infty$ ), one may consider:

$$(8a) \quad \text{Example 3:} \quad \Upsilon(x, z) = \underline{u}(x) + \exp z;$$

$$(8b) \quad \text{Example 4:} \quad \Upsilon(x, z) = \underline{u}(x) + \ln(1 + \exp z).$$

The behavior of the resulting superposition operators is illustrated in Figure 1.

**3.2. The Bregman proximal point algorithm.** The main purpose of this section is to formally derive Algorithm 1. As motivation, we recall the proximal operator [57],  $P: H^1(\Omega) \rightarrow K \cap H_g^1(\Omega)$  and corresponding proximal point algorithm: Given  $u^0 \in H^1(\Omega)$ , define

$$(9) \quad u^k = Pu^{k-1} = \arg \min_{v \in K \cap H_g^1(\Omega)} \left\{ J(v) + \frac{1}{2\alpha^k} \|v - u^{k-1}\|_{H^1(\Omega)}^2 \right\},$$

for each  $k = 1, 2, \dots$

It is well known [57] that the iterates  $u^k = Pu^{k-1}$  converge to the unique fixed point of  $P$ , which coincides with the minimizer of (3). However, computing each iterate  $Pu^{k-1}$  requires

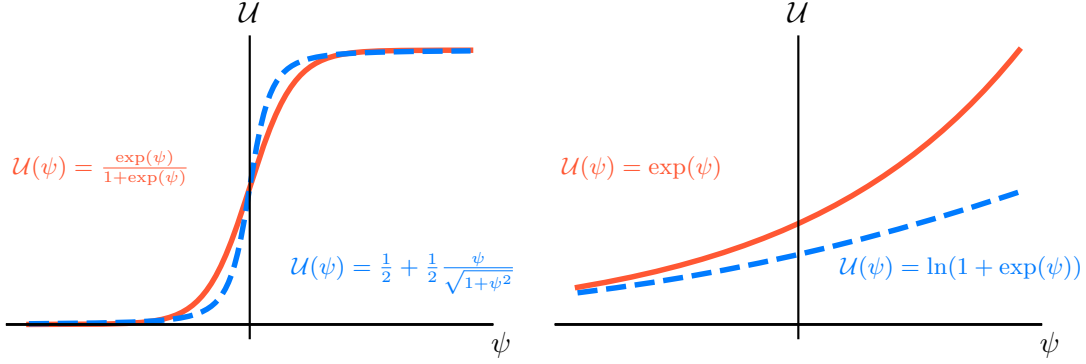


FIGURE 1. Illustration of the different superposition operators  $\mathcal{U}$ . Left:  $\underline{u} = 0$  and  $\bar{u} = 1$ . Right:  $\underline{u} = 0$  and  $\bar{u} = \infty$ .

solving another variational inequality (Euler's inequality, see, e.g., [20, Theorem 7.1-6]): Find  $u^k \in K \cap H_g^1(\Omega)$  such that

$$(10) \quad \frac{1}{\alpha^k} (\nabla(u^k - u^{k-1}), \nabla(v - u^k)) + \frac{1}{\alpha^k} (u^k - u^{k-1}, v - u^k) + (A\nabla u^k, \nabla(v - u^k)) \geq (f, v - u^k),$$

for all  $v \in K \cap H_g^1(\Omega)$ . This renders the standard proximal point method (9) computationally infeasible on this class of problems. Indeed, one would prefer to directly approximate the solution of the original variational inequality (4) instead of solving a sequence of equally challenging problems like (10).

As a remedy, one may consider a particular form of the Bregman proximal point algorithm [46, 61]. The key idea is to replace the squared  $H^1(\Omega)$ -norm in (9) by an alternative *dissimilarity* function:

$$(11) \quad u^k = Pu^{k-1} = \arg \min_{v \in K \cap H_g^1(\Omega)} \left\{ J(v) + \frac{1}{\alpha^k} \int_{\Omega} \mathcal{D}(v, u^{k-1}) \, dx \right\}.$$

Here, the so-called Bregman divergence  $\mathcal{D}(\cdot, \cdot)$  is derived from the error in the first-order Taylor's expansion of a superposition operator denoted  $\mathcal{R}(u)$ . This operator is generated by a Carathéodory function  $R: \Omega \times \mathbb{R} \rightarrow \mathbb{R} \cup \{+\infty\}$  that is strictly convex in its second argument.

More specifically, for a.e.  $x \in \Omega$ , we assume that  $R(x, y)$  maps  $[\underline{u}(x), \bar{u}(x)]$  into  $\mathbb{R}$  and that  $y \mapsto R(x, y)$  is strictly convex and differentiable on the open interval  $(\underline{u}(x), \bar{u}(x))$ . Denoting the corresponding superposition operator  $\mathcal{R}(u)(x) = R(x, u(x))$  and its derivative  $\mathcal{R}'(u)(x) = \frac{\partial}{\partial y} R(x, u(x))$ , we express the Bregman divergence  $\mathcal{D}(\cdot, \cdot)$  as follows [14]:

$$(12) \quad \mathcal{D}(v, u^{k-1}) = \mathcal{R}(v) - \mathcal{R}(u^{k-1}) - \mathcal{R}'(u^{k-1})(v - u^{k-1}).$$

**Example 3.1** (Fermi–Dirac entropy). *Consider the Carathéodory function given by*

$$(13a) \quad R(x, y) = (y - \underline{u}(x)) \ln(y - \underline{u}(x)) + (\bar{u}(x) - y) \ln(\bar{u}(x) - y)$$

*if  $y \in [\underline{u}(x), \bar{u}(x)]$  and  $R(x, y) = +\infty$  otherwise. The corresponding superposition operator,*

$$(13b) \quad \mathcal{R}(u) = (u - \underline{u}) \ln(u - \underline{u}) + (\bar{u} - u) \ln(\bar{u} - u), \quad u \in K,$$

also known as the (generalized) Fermi–Dirac entropy, is continuous over the feasible set  $K$ . Moreover, if  $u \in L^\infty(\Omega)$  with  $\text{ess inf}(\underline{u} - u) > 0$  and  $\text{ess inf}(u - \bar{u}) > 0$ , then

$$(13c) \quad \mathcal{R}'(u) = \ln(u - \underline{u}) - \ln(\bar{u} - u)$$

belongs to  $L^\infty(\Omega)$ .

**3.3. Further properties.** For technical reasons, we require  $R(x, \cdot)$  to have the following supercoercivity property at a.e.  $x \in \Omega$ :

$$(14) \quad R(x, y)/|y| \rightarrow \infty \text{ as } |y| \rightarrow \infty.$$

This ensures that the convex conjugate of  $R(x, \cdot)$  is well-defined over all of  $\mathbb{R}$  [11, 23], see (21a) below. We also require that  $\text{dom } R(x, \cdot) = [\underline{u}(x), \bar{u}(x)]$  to ensure convergence of the iterates (11) to the unique minimizer of  $J$ ; cf. Theorem 5.3 below. Condition 1 is then sufficient to derive Algorithm 1 from (11).

**Condition 1.** For any given  $\varphi \in C_c^\infty(\Omega)$ , there exists a constant  $\delta > 0$  such that the solution  $u^k$  to (11) satisfies

$$(15) \quad u^k \pm \delta\varphi \in K \cap H_g^1(\Omega).$$

This condition can be realized by choosing  $R$  whose derivatives are sufficiently singular at  $\underline{u}$  and  $\bar{u}$  and ensuring that the functions  $f, \underline{u}, \bar{u}$  are sufficiently regular. In particular, if  $f \in L^\infty(\Omega)$  and  $\underline{u}, \bar{u} \in \mathbb{R}$ , then the operators in Examples 3.2 and 3.4 imply Condition 1 [46].

**Example 3.2** (Shannon entropy). The derivation of Algorithm 1 was first given in [46] for the choice

$$(16) \quad \mathcal{R}(u) = u \ln u - u,$$

leading to the (extended) Kullback–Liebler divergence

$$\mathcal{D}(v, u) = v \ln(v/u) - v + u.$$

We refer to [46] for further properties of this setting.

**3.4. From inequality to equality.** The solution of (11) satisfies the following variational inequality: For all  $v \in K \cap H_g^1(\Omega)$ ,

$$(17) \quad \frac{1}{\alpha^k} (\mathcal{R}'(u^k) - \mathcal{R}'(u^{k-1}), v - u^k) + (A\nabla u^k, \nabla(v - u^k)) \geq (f, v - u^k).$$

However, Condition 1 allows us to transform this variational inequality (17) to a variational equation. Indeed, testing (17) with  $v = u^k \pm \delta\varphi$  and rescaling by  $\delta$ , we find that

$$(18) \quad \frac{1}{\alpha^k} (\mathcal{R}'(u^k) - \mathcal{R}'(u^{k-1}), \varphi) + (A\nabla u^k, \nabla\varphi) = (f, \varphi) \quad \forall \varphi \in C_c^\infty(\Omega).$$

**3.5. The latent variable.** We can now formally introduce the latent variable

$$(19) \quad \psi^k = \mathcal{R}'(u^k) \quad \iff \quad (\mathcal{R}')^{-1}(\psi^k) = u^k,$$

where  $\mathcal{R}'$  is invertible because  $\mathcal{R}$  is strictly convex and strictly monotone. Utilizing the sequence of latent variables  $\psi^k$  given by (19) and the density of  $C_c^\infty(\Omega)$  in  $H_0^1(\Omega)$ , we arrive



at the latent variable proximal point method: For each  $k = 1, 2, \dots$ , solve for  $(u^k, \psi^k) \in H_g^1(\Omega) \times L^\infty(\Omega)$  satisfying

$$(20a) \quad \frac{1}{\alpha^k}(\psi^k - \psi^{k-1}, v) + (A\nabla u^k, \nabla v) = (f, v) \quad \forall v \in H_0^1(\Omega),$$

$$(20b) \quad (u^k, \varphi) - ((\mathcal{R}')^{-1}(\psi^k), \varphi) = 0 \quad \forall \varphi \in L^\infty(\Omega).$$

Algorithm 1 is recovered from (20) by setting  $\mathcal{U} = (\mathcal{R}')^{-1}$ , multiplying (20a) by  $\alpha^k$ , and rearranging terms. We note that  $(\psi^k - \psi^{k-1})/\alpha^k$  acts as an approximation to the Lagrange multiplier for the bound constraints in (3b) [46]. It can also be interpreted as a discretized rate of change of the latent gradient flow  $\frac{\partial}{\partial \alpha} \psi = -\nabla J(u)$  over the manifold defined by (19).

**Example 3.3** (Fermi–Dirac entropy, part 2). *Recall the setting of Example 3.1 and observe that*

$$(\mathcal{R}')^{-1}(\psi) = \frac{\underline{u} + \bar{u} \exp \psi}{1 + \exp \psi}.$$

*In turn, notice that  $\mathcal{U}(\psi) = (\mathcal{R}')^{-1}(\psi)$  coincides with the superposition operator generated by (7a).*

**3.6. Duality.** As evident by the derivation above, the generating function  $R$  is closely related to the generating function  $\Upsilon$  in Algorithm 1. This relation is made precise in Proposition 3.1 below, which involves the definition of the convex conjugate of  $R(x, \cdot)$ :

$$(21a) \quad R^*(x, z) = \sup_{y \in \mathbb{R}} \{zy - R(x, y)\}.$$

Likewise, we define the associated superposition operator

$$(21b) \quad \mathcal{R}^*(u)(x) = R^*(x, u(x)).$$

We refer the interested reader to [12] for more general and abstract results.

**Proposition 3.1.** *For a smooth and strictly increasing bijection  $\Upsilon(x, \cdot) : \mathbb{R} \rightarrow (\underline{u}(x), \bar{u}(x))$ , there exists a strictly convex proper function  $R(x, \cdot) : \mathbb{R} \rightarrow \mathbb{R} \cup \{+\infty\}$  such that*

$$(22) \quad \Upsilon(x, z) = \left( \frac{\partial}{\partial y} R(x, \cdot) \right)^{-1} (z) = \frac{\partial}{\partial z} R^*(x, z)$$

*for all  $z \in (\underline{u}(x), \bar{u}(x))$ . Moreover,  $R$  satisfies (14), and the corresponding superposition operators satisfy*

$$(23) \quad \mathcal{U}(\psi) = (\mathcal{R}^*)'(\psi) \quad \forall \psi \in L^\infty(\Omega).$$

*Sketch of proof.* The first equality in (22) follows from the observations that (i) the inverse of a smooth, strictly increasing monotone function is also a smooth, strictly increasing monotone function, and (ii) any smooth, strictly increasing monotone function can be written as the derivative of a convex function. The second equality in (22) follows from the definition of  $R^*$ . Equation (23) follows readily from (22) and the definitions of  $\mathcal{U}$  and  $\mathcal{R}$ . Meanwhile,  $R = (R^*)^*$  satisfies (14) due to [11, Proposition 2.16].  $\square$

**Example 3.4** (Fermi–Dirac entropy, part 3). *We again recall the setting of Example 3.1. Denoting*

$$\Upsilon(x, z) = \left( \frac{\partial}{\partial y} R(x, \cdot) \right)^{-1} (z) = \frac{\underline{u}(x) + \bar{u}(x) \exp z}{1 + \exp z},$$

we recover the function presented in (7a). Further, one can readily derive the expression for  $R^*$ :

$$(24) \quad R^*(x, z) = z\Upsilon(x, z) - R(x, \Upsilon(x, z)).$$

#### 4. SPATIAL DISCRETIZATION

We employ a locally conservative discretization of (6). As a starting point, consider the first-order system formulation of the PDE (6) by introducing the flux variable  $\mathbf{q}^k = -A\nabla u^k$ :

$$(25a) \quad \alpha^k \nabla \cdot \mathbf{q}^k + \psi^k = \alpha^k f + \psi^{k-1} \quad \text{in } \Omega,$$

$$(25b) \quad A^{-1} \mathbf{q}^k + \nabla u^k = 0 \quad \text{in } \Omega,$$

$$(25c) \quad u^k - \mathcal{U}(\psi^k) = 0 \quad \text{in } \Omega.$$

**4.1. Finite element spaces.** In this subsection, we introduce the discrete spaces. On the reference element  $\hat{T}$ , we denote by  $\mathcal{P}_p(\hat{T})$  either the space of all polynomials of degree at most  $p$  ( $\mathbb{P}_p(\hat{T})$ ) if  $\hat{T}$  is simplicial or the space of polynomials of degree at most  $p$  in each direction ( $\mathbb{Q}_p(\hat{T})$ ) if  $\hat{T}$  is a quadrilateral or paralleloptope. We also use the Raviart–Thomas element [56] of degree  $p$  on  $\hat{T}$ ,  $\text{RT}_p(\hat{T}) := [\mathcal{P}_p(\hat{T})]^d + \mathbf{x} \cdot \mathcal{P}_p(\hat{T})$ .

We consider the following finite element spaces:

$$(26a) \quad \Sigma_h^p = \left\{ \mathbf{r}_h \in [L^2(\Omega)]^d : \mathbf{r}_h|_T = \frac{1}{\det \Phi'_T} \Phi'_T \hat{\mathbf{r}} \circ \Phi_T^{-1}, \hat{\mathbf{r}} \in \text{RT}_p(\hat{T}), \forall T \in \mathcal{T}_h \right\},$$

$$(26b) \quad V_h^p = \left\{ v_h \in L^2(\Omega) : v_h|_T = \hat{v} \circ \Phi_T^{-1}, \hat{v} \in \mathcal{P}_p(\hat{T}), \forall T \in \mathcal{T}_h \right\}.$$

The jump of  $v$  on a face  $E \in \mathcal{E}_h$  is defined as

$$[v_h]_{|E} = v_h|_{T_E^1} - v_h|_{T_E^2},$$

where  $E = \partial T_E^1 \cap \partial T_E^2$  and the normal  $\mathbf{n}_E$  is chosen to point from  $T_E^1$  to  $T_E^2$ . This choice is arbitrary. If  $E \subset \partial\Omega$ , then  $[v_h]_{|E}$  is taken as the single valued trace of  $v_h$ . We drop the subscript “ $|E$ ” to simplify notation. The jumps of vector-valued functions are defined similarly.

We define the  $H(\text{div}; \Omega)$  conforming Raviart–Thomas space,

$$(27) \quad \Sigma_{h,\text{div}}^p = \Sigma_h^p \cap H(\text{div}; \Omega) = \{ \mathbf{r}_h \in \Sigma_h^p : [\mathbf{r}_h] \cdot \mathbf{n}_E = 0 \quad \forall E \in \mathcal{E}_h \setminus \partial\Omega \},$$

and we consider the standard discontinuous Galerkin (DG) norm

$$\|v\|_{\text{DG}}^2 = \sum_{T \in \mathcal{T}_h} \|A^{1/2} \nabla v\|_{L^2(T)}^2 + \sum_{E \in \mathcal{E}_h} h_E^{-1} \|[v]\|_{L^2(E)}^2 \quad \forall v \in H^1(\mathcal{T}_h).$$

We also recall the following Poincarè inequality [51, Lemma 3.2], which holds for all  $p \in [1, 6]$  when  $d = 3$  and for all  $p \in [1, \infty)$  when  $d = 2$ ,

$$(28) \quad \|v_h\|_{L^p(\Omega)} \lesssim \|v_h\|_{\text{DG}} \quad \forall v_h \in V_h^p.$$

In what follows, we will make use of the linear lifting operators  $\mathbf{L} : V_h^p \rightarrow \Sigma_{h,\text{div}}^p$  and  $\mathbf{L}_\Gamma : L^2(\partial\Omega) \rightarrow \Sigma_{h,\text{div}}^p$  defined such that

$$(29) \quad (A^{-1}\mathbf{L}(u), \mathbf{r}) = (u, \nabla \cdot \mathbf{r}) \quad \forall \mathbf{r} \in \Sigma_{h,\text{div}}^p,$$

$$(30) \quad (A^{-1}\mathbf{L}_\Gamma(g), \mathbf{r}) = -\langle g, \mathbf{r} \cdot \mathbf{n} \rangle_{\partial\Omega} \quad \forall \mathbf{r} \in \Sigma_{h,\text{div}}^p.$$

**Lemma 4.1.** *Let  $u_h \in V_h^p$  and define  $\mathbf{q}_h = \mathbf{L}(u_h)$  by (29). Then,*

$$(31) \quad \|u_h\|_{\text{DG}} \leq C_L \|A^{-1/2}\mathbf{q}_h\|_{L^2(\Omega)},$$

where  $C_L$  is a mesh-independent positive constant.

*Proof.* The proof follows identically to that of [32, Theorem 3.2] for simplicial meshes. See also a similar result in [22, Theorem 2.3], which covers the parallelotope mesh case.  $\square$

We also introduce the  $L^2$ -projection,  $\Pi_h : H^1(\mathcal{T}_h) \rightarrow V_h^p$ , and we recall the following properties:

$$(32) \quad (\Pi_h v, q_h) = (v, q_h) \quad \forall q_h \in V_h^p, \quad \|\Pi_h v\|_{\text{DG}} \lesssim \|v\|_{\text{DG}}.$$

**4.2. The first-order system proximal Galerkin method.** We are now ready to present the mixed finite element discretization of (6). We start with defining the discrete solutions  $(\mathbf{q}_h^k, u_h^k) \in \Sigma_{h,\text{div}}^p \times V_h^p$  and  $\psi_h^k \in V_h^p$  satisfying the Galerkin discretization of (25):

$$(33a) \quad \alpha^k(\nabla \cdot \mathbf{q}_h^k, v_h) + (\psi_h^k, v_h) = \alpha^k(f, v_h) + (\psi_h^{k-1}, v_h) \quad \forall v_h \in V_h^p,$$

$$(33b) \quad (A^{-1}\mathbf{q}_h^k, \mathbf{v}_h) - (\nabla \cdot \mathbf{v}_h, u_h^k) = -\langle g, \mathbf{v}_h \cdot \mathbf{n} \rangle_{\partial\Omega} \quad \forall \mathbf{v}_h \in \Sigma_{h,\text{div}}^p,$$

$$(33c) \quad (u_h^k, q_h) - (\mathcal{U}(\psi_h^k) + \mathcal{S}(\psi_h^k), q_h) = 0 \quad \forall q_h \in V_h^p.$$

In the above,  $\mathcal{S}$  is an *optional* stabilization/regularization term allowing for additional control over the latent variable  $\psi_h$ . For example, one can choose  $\mathcal{S}(\psi_h^k) = \epsilon\psi_h^k$  for some  $0 \leq \epsilon \ll 1$ . This choice will limit the magnitude of  $\psi_h^k$ , which can reduce the round-off error in the computed solution. We discuss different choices of  $\mathcal{S}$  in Section 7. In what follows, we analyze (33) with  $\mathcal{S} = 0$ .

Using (33c) in (33b) and the fact that  $\nabla \cdot \mathbf{v}_h \in V_h^p$  for any  $\mathbf{v}_h \in \Sigma_{h,\text{div}}^p$ , we arrive at the two-variable formulation of the FOSPG method given in Algorithm 2.

**Remark 1** (The two-variable (34) and three-variable formulations (33)). *Note that (34) is equivalent to (33). This can be immediately observed after defining  $u_h^k = \Pi_h(\mathcal{U}(\psi_h) + \mathcal{S}(\psi_h))$ . We will use this equivalence throughout the paper and refer to the two formulations interchangeably when no confusion arises. Moreover, while the two-variable formulation (34) is more memory efficient than (33), one may compute with both; see, e.g., Algorithm 3 below. The three-variable formulation makes it easier to implement more exotic choices of  $\mathcal{S}(\psi_h)$ , such as  $(\mathcal{S}(\psi_h), q_h) = \epsilon(\nabla_h \psi_h, \nabla_h q_h)$  for some  $0 \leq \epsilon \ll 1$ .*

**Remark 2** (Bound preserving solution  $\mathcal{U}(\psi_h)$  and an average bound preserving solution  $u_h$ ). *In addition to the bound preserving discrete solution  $\mathcal{U}(\psi_h)$ , we obtain a solution  $u_h$  that has bound preserving local averages whenever  $(\mathcal{S}(\psi_h), 1)_T = 0$ . Indeed, testing (33c) with the indicator function of one element  $T \in \mathcal{T}_h$ , we obtain that*

$$(35) \quad \frac{1}{|T|} \int_T u_h \, dx = \frac{1}{|T|} \int_T \mathcal{U}(\psi_h) \, dx, \quad \forall T \in \mathcal{T}_h.$$

**Algorithm 2** The First-Order System Proximal Galerkin Method

- 
- 1: **input:** A discrete latent solution guess  $\psi_h^0 \in V_h^p$  and a sequence of positive step sizes  $\{\alpha^k\}$ .
  - 2: **output:** A bound-preserving approximate solution  $\mathcal{U}(\psi_h) \approx u$  and a locally-conservative flux approximation  $\mathbf{q}_h \approx -A\nabla u$ .
  - 3: Initialize  $k = 1$ .
  - 4: **repeat**
  - 5:   Solve the following (nonlinear) discrete saddle-point problem: Find  $(\mathbf{q}_h, \psi_h) \in \Sigma_{h,\text{div}}^p \times V_h^p$  such that
 
$$(34a) \quad (A^{-1}\mathbf{q}_h, \mathbf{v}_h) - (\nabla \cdot \mathbf{v}_h, \mathcal{U}(\psi_h) + \mathcal{S}(\psi_h)) = -\langle g, \mathbf{v}_h \cdot \mathbf{n} \rangle_{\partial\Omega} \quad \forall \mathbf{v}_h \in \Sigma_{h,\text{div}}^p,$$

$$(34b) \quad \alpha^k (\nabla \cdot \mathbf{q}_h, v_h) + (\psi_h, v_h) = \alpha^k (f, v_h) + (\psi_h^{k-1}, v_h) \quad \forall v_h \in V_h^p.$$
  - 6:   Assign  $\psi_h^k \leftarrow \psi_h$  and  $k \leftarrow k + 1$ .
  - 7: **until** a convergence test is satisfied.
- 

Therefore, if  $\underline{u}, \bar{u} \in \mathbb{R}$ , we obtain that

$$(36) \quad \underline{u} < \frac{1}{|T|} \int_T u_h \, dx < \bar{u}, \quad \forall T \in \mathcal{T}_h.$$

Such a property is useful if one chooses to post-process  $u_h$ ; see Remark 9 for further insight and a numerical example.

**Theorem 4.2** (Existence and uniqueness of solutions). *For all  $k \geq 1$ , there exists a unique solution to (33) and to (34).*

*Proof.* For simplicity, we denote  $\tilde{f} = f + (1/\alpha^k)\psi_h^{k-1}$  and drop the superscript  $k$ . Recall that  $\mathcal{U} = (\mathcal{R}^*)'$  where  $\mathcal{R}^*$  is given in (21b). We then consider the following minimization problem:

$$(37) \quad \inf_{\mathbf{v}_h \in \Sigma_{h,\text{div}}^p} L(\mathbf{v}_h); \quad L(\mathbf{v}_h) = \frac{1}{2} \|A^{-1/2}\mathbf{v}_h\|_{L^2(\Omega)}^2 + \int_{\Omega} \mathcal{R}^*(\Pi_h \tilde{f} - \nabla \cdot \mathbf{v}_h) \, dx + \langle g, \mathbf{v}_h \cdot \mathbf{n} \rangle_{\partial\Omega},$$

where we recall that  $\Pi_h$  is the  $L^2$ -projection onto  $V_h^p$ , see (32). As we show below, (37) admits a solution  $\mathbf{q}_h$  because  $L$  is convex, continuous, and coercive [20, Theorem 9.3–1].

Coercivity follows from the convexity of  $\mathcal{R}^*$  and equivalence of norms in finite dimensions. Indeed, by the subgradient inequality,

$$\int_{\Omega} \mathcal{R}^*(\Pi_h \tilde{f} - \nabla \cdot \mathbf{v}_h) \, dx \geq \int_{\Omega} \mathcal{R}^*(\Pi_h \tilde{f}) \, dx - \int_{\Omega} (\mathcal{R}^*)'(\Pi_h \tilde{f}) \nabla \cdot \mathbf{v}_h \, dx.$$

Hence, with Cauchy–Schwarz inequality and a local trace estimate, we bound  $L(\mathbf{v}_h)$  as follows

$$(38) \quad L(\mathbf{v}_h) \geq \frac{1}{2} \|A^{-1/2}\mathbf{v}_h\|_{L^2(\Omega)}^2 + \int_{\Omega} \mathcal{R}^*(\Pi_h \tilde{f}) \, dx \\ - \|(\mathcal{R}^*)'(\Pi_h \tilde{f})\|_{L^2(\Omega)} \|\nabla \cdot \mathbf{v}_h\|_{L^2(\Omega)} - C_{\text{tr}} \left( \max_{E \subset \partial\Omega} h_E^{-1/2} \right) \|g\|_{L^2(\partial\Omega)} \|\mathbf{v}_h\|_{L^2(\Omega)}.$$

Therefore, from the equivalence of norms in finite dimensions, we deduce that  $L(\mathbf{v}_h) \rightarrow \infty$  as  $\|\mathbf{v}_h\|_{L^2(\Omega)} \rightarrow \infty$ . This establishes the existence of a solution. The uniqueness of the solution follows the strict convexity of  $L$ .

The solution of (37),  $\mathbf{q}_h \in \Sigma_{h,\text{div}}^p$ , satisfies the following optimality condition:

$$(L'(\mathbf{q}_h), \mathbf{v}_h) = (A^{-1}\mathbf{q}_h, \mathbf{v}_h) - \int_{\Omega} (\mathcal{R}^*)'(\Pi_h \tilde{f} - \nabla \cdot \mathbf{q}_h) \nabla \cdot \mathbf{v}_h \, dx + \langle g, \mathbf{v}_h \cdot \mathbf{n} \rangle_{\partial\Omega} = 0.$$

Define  $\psi_h \in V_h^p$  and  $u_h \in V_h^p$  as

$$(39) \quad \psi_h = \alpha \Pi_h \tilde{f} - \alpha \nabla \cdot \mathbf{q}_h, \quad u_h = \Pi_h(\mathcal{U}(\psi_h)).$$

It then easily follows that  $(\mathbf{q}_h, u_h, \psi_h) \in \Sigma_{h,\text{div}}^p \times V_h^p \times V_h^p$  is the unique solution to (33).  $\square$

For each  $k$ , we show a stability estimate with respect to the mesh size  $h$ . To this end, we define the following dual norm:

$$(40) \quad \|v\|_{H^1(\mathcal{T}_h)^*} = \sup_{w \in H^1(\mathcal{T}_h)} \frac{(v, w)}{\|w\|_{\text{DG}}} \quad \forall v \in L^2(\Omega).$$

The stability result we provide below depends on the choice of  $\mathcal{U}$ . To this end, observe that (7a) and (7b) can be written in the following form:

$$(41) \quad \mathcal{U}(\psi)(x) = \Upsilon(x, \psi(x)) = \phi_0(x) \Upsilon_0(\psi(x)) + \phi_1(x),$$

where  $\phi_0, \phi_1 \in L^\infty(\Omega)$  with  $\phi_0(x) \geq \underline{\phi}_0 > 0$  a.e. in  $\Omega$  for some positive constant  $\underline{\phi}_0$  and  $\Upsilon_0: \mathbb{R} \rightarrow (-1, 1)$  is a monotonically increasing bijection with  $\Upsilon_0(0) = 0$  and  $\lim_{z \rightarrow \pm\infty} \Upsilon_0(z) = \pm 1$ . In particular, for examples (7a) and (7b), we have  $\phi_0 = 1/2(\bar{u} - \underline{u})$  and  $\phi_1 = 1/2(\bar{u} + \underline{u})$ .

**Lemma 4.3** (Stability). *For simplicity, assume that the boundary data  $g = 0$  (see Remark 3 for a discussion on the general case). Consider two cases:*

*(Double obstacle problem). If  $\mathcal{U}$  takes the form (41),  $\phi_0 \in L^\infty(\Omega)$  with  $\phi_0(x) \geq \underline{\phi}_0 > 0$  a.e. in  $\Omega$ , and  $\phi_1 \in H_0^1(\Omega)$ , then for any  $k \geq 1$  the solution  $(\mathbf{q}_h^k, u_h^k, \psi_h^k) \in \Sigma_{h,\text{div}}^p \times V_h^p \times V_h^p$  to (33) satisfies*

$$(42) \quad \|A^{-1}\mathbf{q}_h^k\|_{L^2(\Omega)} + \|u_h^k\|_{\text{DG}} + \|\psi_h^k\|_{H^1(\mathcal{T}_h)^*} + \underline{\phi}_0 \|\psi_h^k\|_{L^1(\Omega)} \\ \lesssim \|f\|_{L^2(\Omega)} + \|\psi_h^{k-1}\|_{H^1(\mathcal{T}_h)^*} + \|\nabla \phi_1\|_{L^2(\Omega)} + |\Omega|.$$

*(Anisotropic diffusion). If  $\underline{u}, \bar{u} \in \mathbb{R}$  with  $\underline{u} < 0 < \bar{u}$ , then for any  $k \geq 1$  the solution  $(\mathbf{q}_h^k, u_h^k, \psi_h^k) \in \Sigma_{h,\text{div}}^p \times V_h^p \times V_h^p$  to (33) satisfies*

$$(43) \quad \|A^{-1}\mathbf{q}_h^k\|_{L^2(\Omega)} + \|u_h^k\|_{\text{DG}} + \|\psi_h^k\|_{H^1(\mathcal{T}_h)^*} + \min(-\underline{u}, \bar{u}) \|\psi_h^k\|_{L^1(\Omega)} \\ \lesssim \|f\|_{L^2(\Omega)} + \|\psi_h^{k-1}\|_{H^1(\mathcal{T}_h)^*} + |\Omega|.$$

The hidden constants above are independent of  $h$  but depend on the choice of  $\mathcal{U}$ .

Before providing the proof, we remark on the assumptions.

**Remark 3.** *For non-homogenous boundary data  $g \in H^{1/2}(\partial\Omega)$ , one can consider a lift  $w \in H_0^1(\Omega)$  and set  $u_g = u + w$  where  $u$  solves the homogenous problem. The discrete solution  $u_{h,g}$  is then given by  $u_{h,g} = u_h + \mathcal{I}_h w_g$ , where  $\mathcal{I}_h$  is a suitable quasi-interpolation operator that preserves the boundary data, see for example [27]. Stability estimates for the approximation  $(u_{h,g}, \mathbf{q}_{h,g}) = (u_h + \mathcal{I}_h w_g, \mathbf{q}_h - A \nabla \mathcal{I}_h w_g)$  of  $(u_g, -A \nabla u_g)$  will follow from the triangle inequality, the stability of  $(u_h, \mathbf{q}_h)$ , and the stability properties of the interpolant  $\mathcal{I}_h$ . Moreover, the assumption  $\underline{u} < 0 < \bar{u}$  appears to be a limitation of the current theory. In practice, setting  $\underline{u} = 0$  can be numerically stable, as evidenced by the numerical experiment in Example 7.4.*

*Proof.* (Lemma 4.3) As in the proof of Theorem 4.2, we denote  $\tilde{f} = f + (1/\alpha^k)\psi_h^{k-1}$  and drop the superscript  $k$ . We provide a detailed proof for the double obstacle problem case, and we discuss the modifications to the proof for the anisotropic diffusion case at the end.

We test (33a) with  $v_h = u_h$ , (33b) with  $\mathbf{v}_h = \mathbf{q}_h$ , and (33c) with  $q_h = -\psi_h$ , then we add the resulting equalities. This delivers

$$(44) \quad \alpha \|A^{-1/2} \mathbf{q}_h\|_{L^2}^2 + (\phi_0 \Upsilon_0(\psi_h), \psi_h) = \alpha(\tilde{f}, u_h) - (\phi_1, \psi_h).$$

Observe that since  $\Upsilon_0$  is monotone,  $\Upsilon_0(0) = 0$ , and  $\phi_0 \geq \underline{\phi}_0 > 0$ , the second term in (44) is positive. In addition, we have that

$$\Upsilon_0(\psi_h)\psi_h \geq |\psi_h| - b \quad \text{a.e. in } \Omega,$$

where  $b = \min_{z \in \mathbb{R}} (z\Upsilon_0(z) - |z|) < 0$ . Note that  $b$  is well defined since  $\lim_{z \rightarrow \pm\infty} (z\Upsilon_0(z) - |z|) = 0$ . Therefore,  $b$  is the minimum value of a continuous function over some bounded interval. We arrive at

$$(45) \quad \alpha \|A^{-1/2} \mathbf{q}_h\|_{L^2(\Omega)}^2 + \underline{\phi}_0 \|\psi_h\|_{L^1(\Omega)} \leq \alpha(\tilde{f}, u_h) - (\phi_1, \psi_h) + (b, 1).$$

Proceeding, we bound the terms on the right-hand side of (45). With the Cauchy–Schwarz inequality and (40), we deduce that

$$(46) \quad \begin{aligned} |(\tilde{f}, u_h)| &\leq \alpha \|f\|_{L^2(\Omega)} \|u_h\|_{L^2(\Omega)} + \|\psi_h^{k-1}\|_{H^1(\mathcal{T}_h)^*} \|u_h\|_{\text{DG}} \\ &\leq (\alpha C_L C_p \|f\|_{L^2(\Omega)} + C_L \|\psi_h^{k-1}\|_{H^1(\mathcal{T}_h)^*}) \|A^{-1} \mathbf{q}_h\|_{L^2(\Omega)}. \end{aligned}$$

The last bound follows from first applying Poincaré’s inequality (28) and Lemma 4.1, where we recall the definition of  $\mathbf{L}_h$  (29) and that  $u_h$  satisfies (33b). The second term in (45) is bounded as follows:

$$(47) \quad (\phi_1, \psi_h) \leq \|\psi_h\|_{H^1(\mathcal{T}_h)^*} \|\phi_1\|_{\text{DG}} = \|\psi_h\|_{H^1(\mathcal{T}_h)^*} \|A^{1/2} \nabla \phi_1\|_{L^2(\Omega)},$$

where the last equality follows since  $\phi_1 \in H_0^1(\Omega)$ . The next step consists of bounding  $\|\psi_h\|_{H^1(\mathcal{T}_h)^*}$ . To this end, we use the  $L^2$ -projection and estimate

$$(48) \quad \|\psi_h\|_{H^1(\mathcal{T}_h)^*} = \sup_{w \in H^1(\mathcal{T}_h)} \frac{(\psi_h, w)}{\|w\|_{\text{DG}}} = \sup_{w \in H^1(\mathcal{T}_h)} \frac{(\psi_h, \Pi_h w)}{\|w\|_{\text{DG}}} \lesssim \sup_{w \in H^1(\mathcal{T}_h)} \frac{|(\psi_h, \Pi_h w)|}{\|\Pi_h w\|_{\text{DG}}}.$$

Considering (33a), we write

$$\begin{aligned} (\psi_h, \Pi_h w) &= \alpha(\tilde{f}, \Pi_h w) - \alpha(\nabla \cdot \mathbf{q}_h, \Pi_h w) \\ &= \alpha(\tilde{f}, \Pi_h w) + \alpha(\mathbf{q}_h, \nabla_h(\Pi_h w)) - \sum_{E \in \mathcal{E}_h} \int_E \mathbf{q}_h \cdot \mathbf{n}_E [\Pi_h w] \, ds. \end{aligned}$$

In the last equality, we used that  $[\mathbf{q}_h] \cdot \mathbf{n}_E = 0$ . Therefore, we can bound

$$(49) \quad \begin{aligned} |(\psi_h, \Pi_h w)| &\leq \alpha \|f\|_{L^2(\Omega)} \|\Pi_h w\|_{L^2(\Omega)} + \|\psi_h^{k-1}\|_{H^1(\mathcal{T}_h)^*} \|\Pi_h w\|_{\text{DG}} \\ &\quad + \alpha \|\mathbf{q}_h\|_{L^2(\Omega)} \|\nabla_h(\Pi_h w)\|_{L^2(\Omega)} + C_{\text{tr}} \|\mathbf{q}_h\|_{L^2(\Omega)} \|\Pi_h w\|_{\text{DG}}. \end{aligned}$$

In the above, the constant  $C_{\text{tr}}$  results from applying a local discrete trace inequality to handle the last term. Therefore, along with Poincaré’s inequality (28), (48), and (49), we conclude that

$$(50) \quad \|\psi_h\|_{H^1(\mathcal{T}_h)^*} \leq \alpha C_P \|f\|_{L^2(\Omega)} + \|\psi_h^{k-1}\|_{H^1(\mathcal{T}_h)^*} + (C_{\text{tr}} + \alpha) \|\mathbf{q}_h\|_{L^2(\Omega)}.$$

The bounds on  $\|A^{-1/2}\mathbf{q}_h\|$  and  $\|\psi_h\|_{L^1(\Omega)}$  in (42) follow by applying (50), (47), and (46) to (45). Equation (50) gives the missing bound on  $\|\psi_h\|_{H^1(\mathcal{T}_h)^*}$ . Meanwhile, an application of Lemma 4.1 gives the required bound on  $\|u_h\|_{\text{DG}}$ .

If  $\underline{u}, \bar{u} \in \mathbb{R}$ , then  $\phi_1 \in \mathbb{R}$ . Thus, the equality in (47) no longer holds, and the DG norm of a constant depends inversely on the mesh size. In this case, we remove the dependence on  $\phi_1$  by shifting the problem as follows. Since  $\underline{u} < 0 < \bar{u}$  and since  $\mathcal{U}$  is smooth and monotone, there exists a unique  $c \in \mathbb{R}$  such that  $\mathcal{U}(c) = 0$  by the intermediate value theorem. Set  $\tilde{\psi}_h = \psi_h - c$  and  $\tilde{\mathcal{U}}(z) = \mathcal{U}(z + c)$ ,  $z \in \mathbb{R}$ . Then, the solution  $(\mathbf{q}_h, u_h, \tilde{\psi}_h) \in \Sigma_{h,\text{div}}^p \times V_h^p \times V_h^p$  satisfies

$$(51a) \quad \alpha(\nabla \cdot \mathbf{q}_h, v_h) + (\tilde{\psi}_h, v_h) = \alpha(\tilde{f} - c, v_h) \quad \forall v_h \in V_h^p,$$

$$(51b) \quad (A^{-1}\mathbf{q}_h, \mathbf{v}_h) - (\nabla \cdot \mathbf{v}_h, u_h) = 0 \quad \forall \mathbf{v}_h \in \Sigma_{h,\text{div}}^p,$$

$$(51c) \quad (u_h, q_h) - (\tilde{\mathcal{U}}(\tilde{\psi}_h), q_h) = 0 \quad \forall q_h \in V_h^p.$$

From here, the arguments follow in the same manner as before, where we use that

$$\tilde{\mathcal{U}}(\tilde{\psi}_h)\tilde{\psi}_h \geq a|\tilde{\psi}_h| - b,$$

with  $a = \min(-\underline{u}, \bar{u}) > 0$  and  $b = \min_{z \in \mathbb{R}}(z\tilde{\mathcal{U}}(z) - a|z|)$ . The final bounds on the norms of  $\psi_h$  then follow from the triangle inequality.  $\square$

**4.3. The hybridized first-order system proximal Galerkin method.** An appealing way to reduce the computational cost of FOSPG is through hybridization [13, 6]. After static condensation, this leads to symmetric positive definite linear systems for each linearized subproblem.

On the reference facet  $\hat{E}$ , we denote by  $\mathcal{P}_p(\hat{E})$  the set of all polynomials of degree at most  $k$  on  $\hat{E}$  for  $d = 2$ . For  $d = 3$  and for quadrilateral elements, we set  $\mathcal{P}_p(\hat{E}) = \mathbb{Q}_p(\hat{E})$ . Consider the following space of polynomials defined locally on each facet  $E \in \mathcal{E}_h$

$$(52) \quad M_{h,g}^p = \left\{ \mu_h \in L_2(\mathcal{E}_h) : \begin{aligned} \mu_h|_E &= \hat{\mu} \circ \Phi_E^{-1}, \hat{\mu} \in \mathcal{P}_p(\hat{E}), \forall E \in \mathcal{E}_h \\ \mu|_{E'} &= P_p(g)|_{E'}, \forall E' \subset \partial\Omega \end{aligned} \right\},$$

where  $P_p(g)|_{E'}$  is the  $L^2$ -projection of the Dirichlet boundary data  $g$  onto the polynomial space  $\mathcal{P}_p(E')$ .

Following [24], we consider the following energy norm. For  $\mathbf{q} \in L^2(\Omega)^d$ ,  $v \in H^1(\mathcal{T}_h)$  and  $\hat{v} \in L^2(\partial\mathcal{T}_h)$ , define

$$(53) \quad \|\!(\mathbf{q}, v, \hat{v})\!\|^2 = \|A^{-1/2}\mathbf{q}\|_{\mathcal{T}_h}^2 + \|A^{1/2}\nabla_h v\|_{\mathcal{T}_h}^2 + \sum_{T \in \mathcal{T}_h} h_T^{-1} \|v - \hat{v}\|_{L^2(\partial T)}^2.$$

From the triangle inequality and mesh regularity, see the derivation of [50, Bound 2.20] for details, we remark that for any  $v \in H^1(\mathcal{T}_h)$ ,  $\mathbf{q} \in L^2(\mathcal{T}_h)^d$  and  $q \in L^2(\partial\mathcal{T}_h)$  with  $q = 0$  on  $\partial\Omega$ ,

$$(54) \quad \|v\|_{\text{DG}} \lesssim \|\!(\mathbf{q}, v, q)\!\|.$$

The hybrid mixed discretization relies on a bilinear form  $\mathcal{B}_h : \Sigma_h^p \times H^1(\mathcal{T}_h) \times L^2(\partial\mathcal{T}_h) \rightarrow \mathbb{R}$  to reimpose the continuity of the normal fluxes over the facets, see [24] for more details,

$$(55) \quad \mathcal{B}_h(\mathbf{q}_h, (v, \hat{v})) = (\mathbf{q}_h, \nabla_h v)_h - (v - \hat{v}, \mathbf{q}_h \cdot \mathbf{n})_{\partial\mathcal{T}_h}.$$

**Algorithm 3** The Hybridized First Order System Proximal Galerkin Method

- 
- 1: **input:** A discrete latent solution guess  $\psi_h^0 \in V_h^p$  and a sequence of positive step sizes  $\{\alpha^k\}$ .
  - 2: **output:** A bound-preserving approximate solution  $\mathcal{U}(\psi_h) \approx u$ , a piecewise-polynomial approximate solution  $u_h \approx u$ , and a locally-conservative flux approximation  $\mathbf{q}_h \approx -A\nabla u$ .
  - 3: Initialize  $k = 1$ .
  - 4: **repeat**
  - 5: Solve the following (nonlinear) discrete saddle-point problem: Find  $(\mathbf{q}_h^k, u_h^k, \hat{u}_h^k) \in \Sigma_h^p \times V_h^p \times M_{h,g}^p$  and  $\psi_h^k \in V_h^p$  such that
    - (59a)  $-\alpha^k \mathcal{B}_h(\mathbf{q}_h^k, (v_h, \hat{v}_h)) + (\psi_h^k, v_h) = \alpha^k (f, v_h) + (\psi_h^{k-1}, v_h) \quad \forall (v_h, \hat{v}_h) \in V_h^p \times M_{h,0}^p,$
    - (59b)  $(A^{-1} \mathbf{q}_h^k, \mathbf{v}_h) + \mathcal{B}_h(\mathbf{v}_h, (u_h^k, \hat{u}_h^k)) = 0 \quad \forall \mathbf{v}_h \in \Sigma_h^p,$
    - (59c)  $(u_h^k, q_h) - (\mathcal{U}(\psi_h^k) + \mathcal{S}(\psi_h^k), q_h) = 0 \quad \forall q_h \in V_h^p.$
  - 6: Assign  $k \leftarrow k + 1$ .
  - 7: **until** a convergence test is satisfied.
- 

We also define the following form  $\mathcal{A}_h : (\Sigma_h^p \times V_h^p \times M_{h,0}^p)^2 \rightarrow \mathbb{R}$ :

$$(56) \quad \mathcal{A}_h((\mathbf{q}_h, u_h, \hat{u}_h), (\mathbf{r}_h, v_h, \hat{v}_h)) = (A^{-1} \mathbf{q}_h, \mathbf{r}_h)_{\mathcal{T}_h} + \mathcal{B}_h(\mathbf{r}_h, (u_h, \hat{u}_h)) - \mathcal{B}_h(\mathbf{q}_h, (v_h, \hat{v}_h)).$$

**Lemma 4.4** (Properties of  $\mathcal{A}_h$ ). *For all  $(\mathbf{q}_h, u_h, \hat{u}_h) \in \Sigma_h^p \times V_h^p \times M_{h,0}^p$ , there exists  $\mathbf{r}_h \in \Sigma_h^p$  such that*

$$(57) \quad \mathcal{A}_h((\mathbf{q}_h, u_h, \hat{u}_h), (\mathbf{r}_h, u_h, \hat{u}_h)) \gtrsim \|(\mathbf{q}_h, u_h, \hat{u}_h)\|^2.$$

Further, the form  $\mathcal{A}_h$  is continuous over  $\Sigma_h^p \times V_h^p \times M_{h,0}^p$

$$(58) \quad \mathcal{A}_h((\mathbf{q}_h, u_h, \hat{u}_h), (\mathbf{r}_h, v_h, \hat{v}_h)) \lesssim \|(\mathbf{q}_h, u_h, \hat{u}_h)\| \|(\mathbf{r}_h, v_h, \hat{v}_h)\|$$

*Proof.* The proof closely follows [24]; we provide details in Appendix A for completeness.  $\square$

We are now ready to present the hybridized FOSPG method, given in Algorithm 3.

**Theorem 4.5** (Existence and uniqueness of solutions). *For all  $k \geq 1$ , there exists a unique solution to (59).*

*In addition, if the assumptions of Lemma 4.3 hold, then the solution  $(\mathbf{q}_h^k, u_h^k, \hat{u}_h^k, \psi_h^k) \in \Sigma_h^p \times V_h^p \times M_{h,g}^p \times V_h^p$  to (59) satisfies the stability bounds (42)–(43) with  $\|(\mathbf{q}_h^k, u_h^k, \hat{u}_h^k)\|$  replacing  $(\|A^{-1} \mathbf{q}_h^k\|_{L^2(\Omega)} + \|u_h^k\|_{\text{DG}})$ .*

*Proof.* The proof relies on showing the uniqueness of solutions to (59) and that the solution to (33), guaranteed by Theorem 4.2, defines the solution to (59). As in the proof of Theorem 4.2, we denote  $\tilde{f} = f + (1/\alpha^k)\psi_h^{k-1}$  and drop the superscript  $k$ . Suppose that we are given two solutions  $(\mathbf{q}_h^1, u_h^1, \hat{u}_h^1, \psi_h^1)$  and  $(\mathbf{q}_h^2, u_h^2, \hat{u}_h^2, \psi_h^2)$  to (59). Denote by  $(\boldsymbol{\xi}_h, \xi_h, \hat{\xi}_h) = (\mathbf{q}_h^1, u_h^1, \hat{u}_h^1) - (\mathbf{q}_h^2, u_h^2, \hat{u}_h^2)$ . Then, utilizing the definition of  $\mathcal{A}_h(\cdot, \cdot)$ , we obtain that

$$(60) \quad \alpha \mathcal{A}_h((\boldsymbol{\xi}_h, \xi_h, \hat{\xi}_h), (\mathbf{v}_h, v_h, \hat{v}_h)) + (\psi_h^1 - \psi_h^2, v_h) = 0,$$

$$(61) \quad (\xi_h, q_h) - (\mathcal{U}(\psi_h^1) - \mathcal{U}(\psi_h^2), q_h) = 0,$$



for all  $(\mathbf{v}_h, v_h, \hat{v}_h, q_h) \in \Sigma_h^p \times V_h^p \times M_{h,0}^p \times V_h^p$ . Testing (60) by  $(\mathbf{v}_h, \xi_h, \hat{\xi}_h)$  and (61) by  $\psi_h^1 - \psi_h^2$  and subtracting yields

$$\alpha \mathcal{A}_h((\xi_h, \xi_h, \hat{\xi}_h), (\mathbf{v}_h, \xi_h, \hat{\xi}_h)) + (\mathcal{U}(\psi_h^1) - \mathcal{U}(\psi_h^2), \psi_h^1 - \psi_h^2) = 0,$$

for all  $\mathbf{v}_h \in \Sigma_h^p$ . Using the strict monotonicity of  $\mathcal{U}$  and Lemma 4.4, we conclude that  $(\xi_h, \xi_h, \hat{\xi}_h) = (\mathbf{0}, 0, 0)$ . From (60), we further obtain that  $\psi_h^1 = \psi_h^2$ . Hence, (59) must have unique solutions.

It is standard to show that the solution to (33) defines the solution to (59). Indeed, since

$$\mathcal{B}_h(\mathbf{q}_h, (v_h, \hat{v}_h)) = -(\nabla \cdot \mathbf{q}_h, v_h)_{\mathcal{T}_h} + (\hat{v}_h, \mathbf{q}_h \cdot \mathbf{n})_{\partial \mathcal{T}_h},$$

and  $\mathbf{q}_h \in \Sigma_{h,\text{div}}^p$ , (59a) is satisfied. Further, the facet multipliers can be uniquely determined as  $\hat{u}_h = \lambda_h$  on  $E \in \mathcal{E}_h \setminus \partial \Omega$  and  $\hat{u}_h = P_p(g)$  on  $\partial \Omega$  where  $\lambda_h \in M_{h,0}^p$ , see [31, Chapter 5, Lemma 1.1], uniquely solves

$$(62) \quad (\lambda_h, \mathbf{v}_h \cdot \mathbf{n})_{\partial \mathcal{T}_h} = -(A^{-1} \mathbf{q}_h, \mathbf{v}_h) + (\nabla \cdot \mathbf{v}_h, u_h) - \langle g, \mathbf{v}_h \cdot \mathbf{n} \rangle_{\partial \Omega}, \quad \forall \mathbf{v}_h \in \Sigma_h^p,$$

which is a rewrite of (59c).

The proof of the stability estimates follows the same lines as the proof of Lemma 4.3 where we use Lemma 4.4 and (54). We omit the details for brevity.  $\square$

## 5. A QUADRATURE RULE SPACE DISCRETIZATION AND ITS PROPERTIES

In this section, we show that for a quadrature rule space discretization (in the sense of Condition 2 and Remark 4 below), the solution  $u_h^k$  is bound preserving on quadrature points. This property is demonstrated in Section 5.1 and plays a key role in showing that Algorithm 2 converges to the solution of a discrete mixed VI given in (69), see Section 5.2. This convergence result allows us to show a local mass conservation property in Section 5.3 and to derive a priori error estimates for  $p = 0$  in Section 5.4

**5.1. Bound preservation of  $u_h^k$  on quadrature points.** A key feature of the proximal Galerkin method is equality (33c), which allows us to extract distinctive properties for the solution  $u_h^k$ . For example, we recover that  $u_h^k$  has local averages satisfying the bound constraints, see Remark 2.

One can exploit (33c) further. In particular, under certain conditions, bound preservation of  $u_h^k$  on quadrature points can be established. Indeed, consider if one implements the inner products in (33) by a quadrature rule  $\hat{\mathcal{R}}_p := \{(\hat{x}_i, \hat{w}_i) : i = 1, \dots, n_p\}$  with positive weights  $\hat{w}_i > 0$  on  $\hat{T}$  that is exact for  $\mathcal{P}_{2p}(\hat{T})$ . In this case, equality (33c) is approximated by

$$(63) \quad (u_h^k, q_h) - (\mathcal{U}(\psi_h^k), q_h)_h = 0 \quad \forall q_h \in V_h^p,$$

where for all piecewise continuous functions  $f$  and  $g$ ,

$$(64) \quad (f, g)_h := \sum_{T \in \mathcal{T}_h} \sum_{i=1}^{n_p} f(x_i^T) g(x_i^T) \omega_i^T.$$

In the above,  $w_i^T = |T|/|\hat{T}| \hat{w}_i$  and  $x_i^T = \Phi_T(\hat{x}_i)$  for each  $T \in \mathcal{T}_h$ . Note that  $(f, g)_h = (f, g)$  for all  $f, g \in V_h^p$ . For a given element  $T \in \mathcal{T}_h$ , define the polynomial functions  $\psi_i^T$  satisfying

$$(65) \quad \psi_i^T(x_j^T) = \begin{cases} 1 & \text{if } i = j, \\ 0 & \text{otherwise,} \end{cases} \quad \forall 1 \leq j \leq n_p.$$

For example, one can define  $\psi_i^T$  as the Lagrange polynomial with quadrature points as the Lagrange nodes; i.e. (with  $x[m]$  denoting the  $m$ -th Cartesian coordinate of a point  $x \in \mathbb{R}^d$ ),

$$\psi_i^T(x) = \prod_{m=1}^d \prod_{\substack{\ell=1 \\ x_\ell^T[m] \neq x_i^T[m]}}^p \frac{x[m] - x_\ell^T[m]}{x_i^T[m] - x_\ell^T[m]}.$$

**Condition 2.** We say that the discretization of Algorithm 2 or Algorithm 3 is a quadrature rule space discretization if the extension by zero of any polynomial  $\psi_i^T$  that satisfies (65) belongs to the broken polynomial space  $V_h^p$ , i.e.,

$$(66) \quad \psi_i^T \in \mathcal{P}_p(T) \quad \forall 1 \leq i \leq n_p, \quad \forall T \in \mathcal{T}_h.$$

In this section, we will assume that Condition 2 holds. We comment on its validity in the following remark.

**Remark 4** (Validity of Condition 2). *Condition (66) can be easily verified for quadrilateral or hexahedral elements. For example, one can choose  $n_p = (p+1)^d$  with  $(p+1)$  Gauss-Legendre quadrature points in each Cartesian direction of  $\hat{T}$ . Then, the corresponding quadrature rule is exact for  $\mathbb{Q}_{2p+1}(\hat{T})$  and (66) holds. In addition, (66) holds for  $p=0$  for simplicial elements also. For condition (66) to hold for simplicial elements with  $p \geq 1$ , one needs to use an inexact quadrature to evaluate the inner product  $(u_h^k, q_h)$  in (63). We choose not to explore the consequences of that setting here.*

**Lemma 5.1** (Bound preservation of  $u_h^k$  on quadrature points). *If Condition 2 holds, then for any  $k \geq 1$*

$$(67) \quad \underline{u}(x_i^T) < u_h^k(x_i^T) < \bar{u}(x_i^T) \quad \forall 1 \leq i \leq n_p, \quad \forall T \in \mathcal{T}_h.$$

*Proof.* For any  $T \in \mathcal{T}_h$ , one can choose  $q_h|_T = \psi_i^T$  and  $q_h = 0$  elsewhere in (63) thanks to (66). Using that  $(u_h^k, q_h) = (u_h^k, q_h)_h$ , we derive that

$$(68) \quad u_h^k(x_i^T) = \mathcal{U}(\psi_h^k)(x_i^T) \quad \forall 1 \leq i \leq n_p, \quad \forall T \in \mathcal{T}_h.$$

The result follows from the choice of  $\mathcal{U}$ . □

**5.2. Convergence to a discrete mixed VI.** The main goal of this section, realized in Theorem 5.3, is to show that the proximal iterates generated by Algorithm 2 converge to the solution of the following discrete mixed variational inequality.

Find  $(\mathbf{q}_h^*, u_h^*) \in \Sigma_{h,\text{div}}^p \times \Lambda_h$  such that

$$(69a) \quad (A^{-1} \mathbf{q}_h^*, \mathbf{r}_h) - (u_h^*, \nabla \cdot \mathbf{r}_h) = -\langle g, \mathbf{r}_h \cdot \mathbf{n} \rangle \quad \forall \mathbf{r}_h \in \Sigma_{h,\text{div}}^p,$$

$$(69b) \quad (\nabla \cdot \mathbf{q}_h^* - f, v_h - u_h^*) \geq 0 \quad \forall v_h \in \Lambda_h,$$

where we define the closed and convex set

$$\Lambda_h = \{v_h \in V_h^p, \quad \underline{u}(x_i^T) \leq v_h(x_i^T) \leq \bar{u}(x_i^T), \quad \forall 1 \leq i \leq n_p, \quad \forall T \in \mathcal{T}_h\}.$$

**Lemma 5.2.** *There exists a unique solution  $(\mathbf{q}_h^*, u_h^*) \in \Sigma_{h,\text{div}}^p \times \Lambda_h$  to (69).*

*Proof.* Recall the lifting operators (29)-(30), and consider the minimization problem:

$$(70) \quad \min_{u_h \in \Lambda_h} \frac{1}{2} \|A^{-1/2} \mathbf{L}(u_h)\|^2 - (f, u_h) + \langle g, \mathbf{L}(u_h) \cdot \mathbf{n} \rangle.$$

Note that  $\Lambda_h$  is nonempty since by (66)  $\sum_{T \in \mathcal{T}_h} \sum_{i=1}^{n_p} \bar{u}(x_i^T) \psi_i^T \in \Lambda_h$  (here,  $\psi_i^T$  are extended by zero). The above problem is coercive since  $\|\mathbf{L}(\cdot)\|$  defines a norm on  $V_h^p$ <sup>1</sup> and since norms are equivalent in finite dimensions. Therefore, there exists a solution  $u_h^* \in \Lambda_h$  satisfying the variational inequality

$$(71) \quad \mathcal{W} := (A^{-1}\mathbf{L}(u_h^*), \mathbf{L}(v_h - u_h^*)) - (f, v_h - u_h^*) + \langle g, \mathbf{L}(v_h - u_h^*) \cdot \mathbf{n} \rangle \geq 0, \quad \forall v_h \in \Lambda_h.$$

The uniqueness of  $u_h^*$  follows from strict convexity (a composition of a strictly convex function  $\|\cdot\|^2$  with a linear function  $A^{-1/2}\mathbf{L}(\cdot)$  is strictly convex). Defining

$$(72) \quad \mathbf{q}_h^* = \mathbf{L}(u_h^*) + \mathbf{L}_\Gamma(g),$$

we see that (69a) holds and from (71), we derive that

$$\begin{aligned} \mathcal{W} &= (A^{-1}\mathbf{L}(u_h^*), \mathbf{L}(v_h - u_h^*)) - (f, v_h - u_h^*) + (A^{-1}\mathbf{L}_\Gamma(g), \mathbf{L}(v_h - u_h^*)) \\ &= (A^{-1}\mathbf{q}_h^*, \mathbf{L}(v_h - u_h^*)) - (f, v_h - u_h^*) \\ &= (\nabla \cdot \mathbf{q}_h^* - f, v_h - u_h^*) \geq 0. \end{aligned}$$

□

**Remark 5.** *The discrete variational inequality (69) is an approximation of the following mixed variational inequality. Find  $(\mathbf{q}^*, u^*) \in H(\text{div}; \Omega) \times L^2(\Omega)$  such that*

$$(73a) \quad (A^{-1}\mathbf{q}^*, \mathbf{r}) - (u^*, \nabla \cdot \mathbf{r}) = -\langle g, \mathbf{r} \cdot \mathbf{n} \rangle \quad \forall \mathbf{r} \in H(\text{div}; \Omega),$$

$$(73b) \quad (\nabla \cdot \mathbf{q}^* - f, v - u^*) \geq 0 \quad \forall v \in \Lambda,$$

where  $\Lambda \subset L^2(\Omega)$  is given by

$$(74) \quad \Lambda = \{v \in L^2(\Omega), \underline{u} \leq v \leq \bar{u} \text{ a.e. in } \Omega\}.$$

The well-posedness of the above problem can be established by showing that under sufficient regularity assumptions, the solution to (4) defines the solution to (73). We refer to [15] for additional details.

Define the discrete Bregman distance that discretizes the integral of (12)

$$D_h(u_h, v_h) = (\mathcal{R}(u_h) - \mathcal{R}(v_h), 1)_h - (\mathcal{R}'(v_h), u_h - v_h)_h \quad \forall u_h \in \Lambda_h, v_h \in \tilde{\Lambda}_h,$$

where  $\tilde{\Lambda}_h$  is given by

$$\tilde{\Lambda}_h = \{v_h \in V_h^p, \underline{u}(x_i^T) < v_h(x_i^T) < \bar{u}(x_i^T) \quad \forall 1 \leq i \leq n_p, \quad \forall T \in \mathcal{T}_h\}.$$

**Theorem 5.3** (Convergence to the discrete mixed VI). *Assume that condition (66) holds. Then, the proximal iterates  $(\mathbf{q}_h^{k+1}, u_h^{k+1})$  generated by (33) converge to the solution  $(\mathbf{q}_h^*, u_h^*) \in \Sigma_{h,\text{div}}^p \times \Lambda_h$  of the discrete mixed variational inequality (69). Further, the following bound holds for any  $\ell \geq 1$ :*

$$(75) \quad \|u_h^\ell - u_h^*\|_{\text{DG}}^2 + \|A^{-1/2}(\mathbf{q}_h^\ell - \mathbf{q}_h^*)\|_{L^2(\Omega)}^2 \lesssim \frac{D_h(u_h^*, u_h^0)}{\sum_{k=1}^{\ell} \alpha_k},$$

where  $u_h^0 \in V_h^p$  is defined by

$$(u_h^0, q_h) = (\mathcal{U}(\psi_h^0), q_h)_h \quad \forall q_h \in V_h^p.$$

---

<sup>1</sup> $\|\mathbf{L}(\cdot)\|$  defines a norm on  $V_h^p$  since if  $(u_h, \nabla \cdot \mathbf{r}_h) = 0 \quad \forall \mathbf{r}_h \in \Sigma_{h,\text{div}}^p$  then  $u_h = 0$ . This follows from the discrete inf-sup condition, see for e.g. [28, Lemma 51.10].

*Proof. Step 1 (Reformulation).* Considering (68) and recalling that  $\mathcal{U} = (\mathcal{R}')^{-1}$  (22), we have that  $u_h^k \in \tilde{\Lambda}_h$  for all  $k \geq 0$  and that

$$(76) \quad \psi_h^k(x_i^T) = \mathcal{R}'(u_h^k)(x_i^T) \quad \forall 1 \leq i \leq n_p, \forall T \in \mathcal{T}_h.$$

It also follows that for  $u_h, v_h \in \tilde{\Lambda}_h$ , the derivative of  $D_h$  with respect to the first argument is

$$D'_h(u_h, v_h)(w) = (\mathcal{R}'(u_h) - \mathcal{R}'(v_h), w)_h \quad \forall w \in \Lambda_h.$$

The above arguments allow us to write that for any  $v \in \Lambda_h$

$$(77) \quad \frac{1}{\alpha^k}(\psi_h^k - \psi_h^{k-1}, v)_h = \frac{1}{\alpha^k}(\mathcal{R}'(u_h^k) - \mathcal{R}'(u_h^{k-1}), v)_h = \frac{1}{\alpha^k}D'_h(u_h^k, u_h^{k-1})(v).$$

Therefore, from (33a), we deduce that

$$(78) \quad \frac{1}{\alpha^k}D'_h(u_h^k, u_h^{k-1})(v) + (\nabla \cdot \mathbf{q}_h^k, v) - (f, v) = 0 \quad \forall v \in \Lambda_h.$$

Using the lifting operator (29) in (78), we obtain that

$$(79) \quad \frac{1}{\alpha^k}D'_h(u_h^k, u_h^{k-1})(v) + (A^{-1}\mathbf{L}(v), \mathbf{q}_h^k) - (f, v) = 0 \quad \forall v \in \Lambda_h.$$

We now rewrite  $\mathbf{q}_h^k$  using the lifting operators (29)–(30) and (33b):

$$(80) \quad \mathbf{q}_h^k = \mathbf{L}(u_h^k) + \mathbf{L}_\Gamma(g).$$

Substituting the expression (80) for  $\mathbf{q}_h^k$  into (79) and using (30) yields

$$(81) \quad \frac{1}{\alpha^k}D'_h(u_h^k, u_h^{k-1})(v) + (A^{-1}\mathbf{L}(v), \mathbf{L}(u_h^k)) - \langle g, \mathbf{L}(v) \cdot \mathbf{n} \rangle_{\partial\Omega} - (f, v) = 0, \quad \forall v \in \Lambda_h.$$

Since  $u_h^k \in \tilde{\Lambda}_h \subset \Lambda_h$ , we see from the above that  $u_h^k$  solves the following strictly convex and coercive minimization problem:<sup>2</sup>

$$(82) \quad \min_{v \in \Lambda_h} \frac{1}{\alpha^k}D_h(v, u_h^{k-1}) + J_h(v); \quad J_h(v) = \frac{1}{2}(A^{-1}\mathbf{L}(v), \mathbf{L}(v)) - \langle g, \mathbf{L}(v) \cdot \mathbf{n} \rangle_{\partial\Omega} - (f, v).$$

Therefore,  $u_h^k$  is the unique solution to (82). From here, we see that for any  $k \geq 1$

$$(83) \quad J_h(u_h^k) \leq \frac{1}{\alpha^k}D_h(u_h^{k-1}, u_h^{k-1}) + J_h(u_h^{k-1}) = J_h(u_h^{k-1}).$$

*Step 2. (Convergence of  $J_h(u_h^k)$ ).* Here, we adapt the arguments from [46, proof of Theorem 4.13]. We test (81) with  $v = u_h^k$  and with  $v = u_h^* \in \Lambda_h$  and subtract the resulting equations:

$$(84) \quad \frac{1}{\alpha^k}D'_h(u_h^k, u_h^{k-1})(u_h^k - u_h^*) + (A^{-1}\mathbf{L}(u_h^k - u_h^*), \mathbf{L}(u_h^k)) \\ - \langle g, \mathbf{L}(u_h^k - u_h^*) \cdot \mathbf{n} \rangle_{\partial\Omega} - (f, u_h^k - u_h^*) = 0.$$

We readily check that the three points identity [46, Proposition 4.6] also holds for the discrete distance:

$$D'_h(u_h^k, u_h^{k-1})(u_h^k - u_h^*) = D_h(u_h^*, u_h^k) - D_h(u_h^*, u_h^{k-1}) + D_h(u_h^k, u_h^{k-1}).$$

<sup>2</sup>The coercivity of the problem follows from the fact  $D_h(v, u_h^{k-1})$  is always positive and that  $\|\mathbf{L}(\cdot)\|$  defines a norm on  $V_h^p$  since if  $(u_h, \nabla \cdot \mathbf{r}_h) = 0 \forall \mathbf{r}_h \in \Sigma_{h, \text{div}}^p$  then  $u_h = 0$ . This follows from the discrete inf-sup condition.

Using the definition of  $J_h$  and the above in (84), we obtain

$$(85) \quad D_h(u_h^k, u_h^{k-1}) + (D_h(u^*, u_h^k) - D_h(u_h^*, u_h^{k-1})) \\ + \alpha_k \left( J_h(u_h^k) - J_h(u_h^*) + \frac{1}{2} \|A^{-1/2} \mathbf{L}(u_h^k - u_h^*)\|^2 \right) \leq 0.$$

Summing the above from  $k = 1, \dots, \ell$  yields

$$(86) \quad D_h(u^*, u_h^\ell) + \sum_{k=1}^{\ell} D_h(u_h^k, u_h^{k-1}) + \sum_{k=1}^{\ell} \alpha_k (J_h(u_h^k) - J_h(u_h^*)) \leq D_h(u^*, u_h^0).$$

Utilizing (83), we obtain that

$$(87) \quad D_h(u^*, u_h^\ell) + \sum_{k=1}^{\ell} D_h(u_h^k, u_h^{k-1}) + (J_h(u_h^\ell) - J_h(u_h^*)) \sum_{k=1}^{\ell} \alpha_k \leq D_h(u^*, u_h^0).$$

Therefore,

$$(88) \quad J_h(u_h^\ell) \leq J_h(u_h^*) + \frac{D_h(u^*, u_h^0)}{\sum_{k=1}^{\ell} \alpha_k}.$$

*Step 3.* (Convergence of  $\mathbf{q}_h^*$  and  $u_h^*$ ) Using the definitions of  $\mathbf{L}$  and  $\mathbf{L}_\Gamma$  (29)–(30), the discrete solution  $u_h^*$  satisfies

$$(89) \quad (A^{-1} \mathbf{L}(v - u_h^*), \mathbf{L}(u_h^*)) - (f, v - u_h^*) - \langle g, \mathbf{L}(v - u_h^*) \cdot \mathbf{n} \rangle_{\partial\Omega} \geq 0, \quad \forall v \in \Lambda_h.$$

Choosing  $v = u_h^\ell$  and rewriting, the above reads

$$(90) \quad J_h(u_h^\ell) - J_h(u_h^*) - \frac{1}{2} \|A^{-1/2} \mathbf{L}(u_h^\ell - u_h^*)\|^2 \geq 0.$$

Rearranging and using (88), we obtain

$$(91) \quad \frac{1}{2} \|A^{-1/2} \mathbf{L}(u_h^\ell - u_h^*)\|^2 \leq J_h(u_h^\ell) - J_h(u_h^*) \leq \frac{D_h(u^*, u_h^0)}{\sum_{k=1}^{\ell} \alpha_k}.$$

Since  $\mathbf{q}_h^* = \mathbf{L}(u_h^*) + \mathbf{L}_\Gamma(g)$  and  $\mathbf{q}_h^\ell = \mathbf{L}(u_h^\ell) + \mathbf{L}_\Gamma(g)$ , we obtain the required bound on  $\|A^{-1/2}(\mathbf{q}_h^\ell - \mathbf{q}_h^*)\|$ . Utilizing Lemma 4.1, one obtains the required bound on  $\|u_h^\ell - u_h^*\|_{\text{DG}}$ .  $\square$

**5.3. Local mass conservation.** We now show that for a fixed mesh, the iterates of Algorithm 2 converge (with  $\alpha_k$ ) to a discrete solution satisfying a local mass conservation property on elements that do not intersect the obstacle.

**Corollary 1** (Local mass conservation). *Fix  $T \in \mathcal{T}_h$ . If the solution  $u_h^*$  to (69) satisfies*

$$(92) \quad \underline{u} < u_h^* < \bar{u} \quad \text{in } T,$$

*then the following property holds*

$$(93) \quad |(\nabla \cdot \mathbf{q}_h^\ell - f, 1)_T| \lesssim \frac{D_h(u_h^*, u_h^0)}{\sum_{k=1}^{\ell} \alpha_k} h_T^{(2d-3)/2}.$$

*Proof.* Define the discrete function  $\lambda_h^\ell = (\psi_h^{\ell-1} - \psi_h^\ell)/\alpha^\ell \in V_h^p$  for  $\ell \geq 1$ . Further, let  $\lambda_h^* = (\nabla \cdot \mathbf{q}_h^* - f) \in L^2(\Omega)$  be the discrete Lagrange multiplier. Then, considering (33a), we have for any  $v_h \in V_h^p$

$$(\lambda_h^\ell - \lambda_h^*, v_h) = (\nabla \cdot (\mathbf{q}_h^\ell - \mathbf{q}_h^*), v_h) = -(\mathbf{q}_h^\ell - \mathbf{q}_h^*, \nabla v_h) + \sum_{E \in \mathcal{E}_h} \int_E (\mathbf{q}_h - \mathbf{q}_h^*) \cdot \mathbf{n}_E[v_h].$$

Considering (40) and using a similar argument to (48) and Theorem 5.3, we obtain that

$$(94) \quad \|\lambda_h^\ell - \lambda_h^*\|_{H^1(\mathcal{T}_h)^*} \lesssim \|\mathbf{q}_h^\ell - \mathbf{q}_h^*\|_{L^2(\Omega)} \lesssim \frac{D_h(u_h^*, u_h^0)}{\sum_{k=1}^{\ell} \alpha_k}.$$

Now, test (33a) with  $\chi_T$  the indicator function of the element  $T \in \mathcal{T}_h$ :

$$(95) \quad (\nabla \cdot \mathbf{q}_h^\ell - f, 1)_T = (\lambda_h^\ell - \lambda_h^*, \chi_T) + (\lambda_h^*, 1)_T.$$

Observe that if  $T$  satisfies (92), the second term above evaluates to zero. This can be seen from (69b) where we test with  $v_h = u_h^* \pm \delta \chi_T \in \Lambda_h$  for small enough constant  $\delta$ . Namely, one can choose  $\delta = \min(\bar{u} - \max_{\mathbf{x} \in T} u_h^*(\mathbf{x}), \min_{\mathbf{x} \in T} u_h^*(\mathbf{x}) - \underline{u})$ . Bounding the first term in (95) with  $\|\lambda_h^\ell - \lambda_h^*\|_{H^1(\mathcal{T}_h)^*} \|\chi_T\|_{\text{DG}}$ , using that  $\|\chi_T\|_{\text{DG}} \lesssim h_T^{(2d-3)/2}$ , and invoking (94) shows (93).  $\square$

**5.4. A priori error estimates.** Theorem 5.3 allows us to complete the analysis and provide an error estimate between the iterations  $(\mathbf{q}_h^k, u_h^k) \in \Sigma_{h,\text{div}}^p \times \Lambda_h$  and the solution  $(\mathbf{q}^*, u^*) = (-A\nabla u, u)$  of (1). The proof of such a bound follows from the triangle inequality  $\|\mathbf{q}_h^\ell - \mathbf{q}^*\| \leq \|\mathbf{q}_h^\ell - \mathbf{q}_h^*\| + \|\mathbf{q}_h^* - \mathbf{q}^*\|$  and (75) after establishing an estimate for  $\|\mathbf{q}_h^* - \mathbf{q}^*\|$ . In Theorem 5.4, we provide an estimate for the latter error when  $p = 0$ . For  $p \geq 1$ , the convergence of discrete mixed VI (69) requires further investigation.

**Theorem 5.4** (Convergence of the discrete mixed VI for  $p = 0$ ). *Let  $(\mathbf{q}_h^*, u_h^*) \in \Sigma_{h,\text{div}}^0 \times V_h^0$  be the solution to the discrete mixed VI (5.3).*

*(Anisotropic diffusion). If  $\underline{u}, \bar{u} \in \mathbb{R}$  and  $(\mathbf{q}^*, u^*) = (-A\nabla u, u) \in H(\text{div}, \Omega) \times L^2(\Omega)$  where  $u$  solves (1), then*

$$(96) \quad \|u_h^* - u^*\|_{L^2(\Omega)} + \|A^{-1/2}(\mathbf{q}_h^* - \mathbf{q}^*)\|_{L^2(\Omega)} \lesssim \inf_{\mathbf{r}_h \in \Sigma_{h,\text{div}}^0} \|A^{-1/2}(\mathbf{q}^* - \mathbf{r}_h)\|_{L^2(\Omega)} + h\|\nabla \cdot \mathbf{q}^*\|_{L^2(\Omega)} + \inf_{v_h \in V_h^0} \|u_h^* - v_h\|_{L^2(\Omega)}.$$

*(Double obstacle problem). If  $\underline{u}, \bar{u} \in H^2(\Omega)$  and  $(\mathbf{q}^*, u^*) = (-A\nabla u, u) \in H^1(\Omega) \times H^2(\Omega)$  where  $u^*$  solves (3a), then*

$$(97) \quad \|u_h^* - u^*\|_{L^2(\Omega)} + \|A^{-1/2}(\mathbf{q}_h^* - \mathbf{q}^*)\|_{L^2(\Omega)} \lesssim C_{\text{reg}} h,$$

where  $C_{\text{reg}}$  depends on  $\|\mathbf{q}^*\|_{H^1(\Omega)}$ ,  $\|u^*\|_{H^2(\Omega)}$ ,  $\|\underline{u}\|_{H^2(\Omega)}$ ,  $\|\bar{u}\|_{H^2(\Omega)}$ , and  $\|f\|_{L^2(\Omega)}$ .

*Proof.* We make use of the interpolation operator introduced in [26] for simplicial elements that satisfies  $\mathbf{I}_h : H(\text{div}; \Omega) \rightarrow \Sigma_{h,\text{div}}^0$  with

$$(98) \quad (\nabla \cdot \mathbf{I}_h \mathbf{q}^*, v_h) = (\nabla \cdot \mathbf{q}^*, v_h) \quad \forall v_h \in V_h^0,$$

$$(99) \quad \|\mathbf{q}^* - \mathbf{I}_h \mathbf{q}^*\|_{L^2(\Omega)} \lesssim \inf_{\mathbf{r}_h \in \Sigma_{h,\text{div}}^0} \|\mathbf{q}^* - \mathbf{r}_h\|_{L^2(\Omega)} + h\|\nabla \cdot \mathbf{q}^*\|_{L^2(\Omega)}.$$

Note that no additional assumptions on the regularity of  $\mathbf{q}^*$  are needed; see [26, Theorem 3.2]. Considering (69a), we derive that

$$(100) \quad (A^{-1}(\mathbf{q}^* - \mathbf{q}_h^*), \mathbf{r}_h) = (u^* - u_h^*, \nabla \cdot \mathbf{r}_h) \quad \forall \mathbf{r}_h \in \Sigma_{h,\text{div}}^0.$$

The above property and (98) allow us to derive that

$$(101) \quad \|A^{-1/2}(\mathbf{q}^* - \mathbf{q}_h^*)\|_{L^2(\Omega)}^2 = (A^{-1}(\mathbf{q}^* - \mathbf{q}_h^*), \mathbf{q}^* - \mathbf{I}_h \mathbf{q}^*) + (u^* - u_h^*, \nabla \cdot (\mathbf{I}_h \mathbf{q}^* - \mathbf{q}_h^*))$$

Denoting  $\Pi_h u^* \in V_h^0$  as the  $L^2$ -projection onto  $V_h^0$ , there holds

$$(102) \quad \begin{aligned} (u^* - u_h^*, \nabla \cdot (\mathbf{I}_h \mathbf{q}^* - \mathbf{q}_h^*)) &= (\Pi_h u^* - u_h^*, \nabla \cdot (\mathbf{I}_h \mathbf{q}^* - \mathbf{q}_h^*)) \\ &= (\Pi_h u^* - u_h^*, \nabla \cdot \mathbf{q}^* - f) + (\Pi_h u^* - u_h^*, f - \nabla \cdot \mathbf{q}_h^*) \\ &\leq (\Pi_h u^* - u_h^*, \nabla \cdot \mathbf{q}^* - f). \end{aligned}$$

where we used (98) and (69b) with test function  $v_h = \Pi_h u^*$ . We now consider two cases.

*Case 1:* If  $u^*$  solves (1), then the last term above is zero. A simple application of Cauchy–Schwarz inequality for the first term in (101) and the approximation property (99) yields the required bound on  $\|A^{-1/2}(\mathbf{q}_h^* - \mathbf{q}^*)\|_{L^2(\Omega)}$  in (96).

*Case 2:* If  $u^*$  solves (3a), then the result essentially follows from [15, Section 4], which covers the unilateral obstacle case with  $\bar{u} = +\infty$ . Here, we extend the result to the bilateral obstacle case. We further expand (102) and write

$$(103) \quad \begin{aligned} (\Pi_h u^* - u_h^*, \nabla \cdot \mathbf{q}^* - f) &= (\Pi_h u^* - u^*, \nabla \cdot \mathbf{q}^* - f) + (u^* - u_h^*, \nabla \cdot \mathbf{q}^* - f) \\ &\leq (\Pi_h u^* - u^*, \nabla \cdot \mathbf{q}^* - f), \end{aligned}$$

where we used (73b) with test function  $v = u_h^*$ . To estimate the term above, fix an element  $T \in \mathcal{T}_h$  and recall the pointwise relation  $\nabla \cdot \mathbf{q}^* - f = 0$  if  $\underline{u} < u^* < \bar{u}$ . Therefore, we can write

$$(104) \quad (\Pi_h u^* - u^*, \nabla \cdot \mathbf{q}^* - f)_T = (\Pi_h u^* - \underline{u}, \nabla \cdot \mathbf{q}^* - f)_{T_{\underline{u}}} + (\Pi_h u^* - \bar{u}, \nabla \cdot \mathbf{q}^* - f)_{T_{\bar{u}}},$$

where  $T_{\underline{u}} = \{x \in T, u^*(x) = \underline{u}(x)\}$  and  $T_{\bar{u}} = \{x \in T, u^*(x) = \bar{u}(x)\}$ . Suppose that  $|T_{\underline{u}}| \neq 0$  and/or  $|T_{\bar{u}}| \neq 0$ . With the stability of the  $L^2$  projection and triangle inequality, we estimate

$$(105) \quad \begin{aligned} \|\Pi_h u^* - \underline{u}\|_{L^2(T_{\underline{u}})} &\leq \|\Pi_h(u^* - \underline{u})\|_{L^2(T)} + \|\Pi_h \underline{u} - \underline{u}\|_{L^2(T)} \\ &\leq \|u^* - \underline{u}\|_{L^2(T)} + \|\Pi_h \underline{u} - \underline{u}\|_{L^2(T)} \end{aligned}$$

Since  $u^* - \underline{u} = 0$  on  $|T_{\underline{u}}|$ , we use the extended Steklov–Poincaré inequality twice (see [25, Lemma 3.30]) and the approximation properties of  $\Pi_h$  to bound the first and second terms above respectively:

$$\|\Pi_h u^* - \underline{u}\|_{L^2(T_{\underline{u}})} \lesssim h^2(\|u^* - \underline{u}\|_{H^2(T)} + \|\underline{u}\|_{H^2(T)}),$$

Following the same arguments, one obtains a similar bound for  $\|\Pi_h u^* - \bar{u}\|_{L^2(T_{\bar{u}})}$ . Therefore, along with Cauchy–Schwarz inequality and (104), we bound (103) with

$$(106) \quad (\Pi_h u^* - u_h^*, \nabla \cdot \mathbf{q}^* - f) \lesssim h^2(\|u^*\|_{H^2(\Omega)} + \|\underline{u}\|_{H^2(\Omega)} + \|\bar{u}\|_{H^2(\Omega)}) \|\nabla \cdot \mathbf{q}^* - f\|_{L^2(\Omega)}.$$

The bound on  $\|A^{-1/2}(\mathbf{q}_h^* - \mathbf{q}^*)\|_{L^2(\Omega)}$  now follows by using the above in (102) and (101) along with the approximation property  $\|\mathbf{I}_h \mathbf{q}^* - \mathbf{q}^*\|_{\Omega} \lesssim h \|\mathbf{q}^*\|_{1,\Omega}$ .

Finally, the inf-sup stability of the finite element spaces yields the required bounds on  $\|u_h^* - u^*\|_{L^2(\Omega)}$ ; see also [15, Theorem 2.3].  $\square$

## 6. ANALYSIS OF THE LINEARIZED SUB-PROBLEMS FROM NEWTON'S METHOD

The convergence property established in Section 5 relies on condition (66), which holds for  $p = 0$  or for quadrilateral or hexahedral elements with (66) enforced. For general meshes and spaces, we present here an analysis of the stability and convergence properties of the linearized sub-problems resulting from Newton's method. We view this as an important step towards establishing the convergence of the hybrid first-order system proximal Galerkin method and its mesh independence properties.

For simplicity, we drop the superscripts  $k$  to simplify the notation and we only consider the homogeneous problem and its solution. At each step  $k$ , one solves a sequence of linearized subproblems of (59) with Newton's method of the following form:

Given  $\psi \in L^\infty(\Omega)$ ,  $\tilde{f} \in L^2(\Omega)$ ,  $\phi \in H_0^1(\Omega)$  and  $\chi \in L^2(\Omega)$ , find  $(\mathbf{q}_h, u_h, \hat{u}_h) \in \Sigma_h^p \times V_h^p \times M_{h,0}^p$  and  $\delta_h \in V_h^p$  solving

$$(107a) \quad (\delta_h, v_h) - \alpha \mathcal{B}_h(\mathbf{q}_h, (v_h, \hat{v}_h)) = (\tilde{f}, v_h) \quad \forall (v_h, \hat{v}_h) \in V_h^p \times M_{h,0}^p,$$

$$(107b) \quad (A^{-1} \mathbf{q}_h, \mathbf{r}_h) + \mathcal{B}_h(\mathbf{r}_h, (u_h, \hat{u}_h)) = 0 \quad \forall \mathbf{r}_h \in \Sigma_h^p,$$

$$(107c) \quad (u_h, q_h) - (\mathcal{U}'(\psi) \delta_h, q_h) = (\phi + \chi, q_h) \quad \forall q_h \in V_h^p.$$

With the definition of  $\mathcal{A}_h$  (56), we write the above scheme as follows: Find  $(\mathbf{q}_h, u_h, \hat{u}_h) \in \Sigma_h^p \times V_h^p \times M_{h,0}^p$  and  $\delta_h \in V_h^p$  such that

$$(108a) \quad \alpha \mathcal{A}_h((\mathbf{q}_h, u_h, \hat{u}_h), (\mathbf{r}_h, v_h, \hat{v}_h)) + (\delta_h, v_h) = (\tilde{f}, v_h) \quad \forall (\mathbf{r}_h, v_h, \hat{v}_h) \in \Sigma_h^p \times V_h^p \times M_{h,0}^p,$$

$$(108b) \quad (u_h, q_h) - (\mathcal{U}'(\psi) \delta_h, q_h) = (\phi + \chi, q_h) \quad \forall q_h \in V_h^p.$$

**6.1. Stability.** We establish existence and uniqueness and stability estimates for (108). The proof utilizes similar arguments to [13, Section 4.3.2 and Section 5.5.3] and [46, Appendix B]. Since our setting is nonconforming, we provide the details.

**Lemma 6.1** (First stability estimate). *The linearized problem (108) admits a unique solution satisfying*

$$(109) \quad \alpha \|(\mathbf{q}_h, u_h, \hat{u}_h)\| + \|\delta_h\|_{H^1(\mathcal{T}_h)^*} + \|\mathcal{U}'(\psi)^{1/2} \delta_h\|_{L^2(\Omega)} \\ \lesssim \|\tilde{f}\|_{H^1(\mathcal{T}_h)^*} + \|\nabla \phi\|_{L^2(\Omega)} + \|\mathcal{U}'(\psi)^{-1/2} \chi\|_{L^2(\Omega)}.$$

*Proof.* The existence of solutions follows by uniqueness since this is a square linear system. Therefore, it suffices to show the stability estimate.

Testing (108a) with  $(\mathbf{r}_h, u_h, \hat{u}_h)$  where  $\mathbf{r}_h$  satisfies (57) (see Lemma 4.4) and (108b) with  $\delta_h$ , subtracting the resulting equations, and using Cauchy-Schwarz inequality, we obtain

$$(110) \quad \alpha \|(\mathbf{q}_h, u_h, \hat{u}_h)\|^2 + \|\mathcal{U}'(\psi)^{1/2} \delta_h\|_{L^2(\Omega)}^2 \\ \lesssim \|\tilde{f}\|_{H^1(\mathcal{T}_h)^*} \|u_h\|_{\text{DG}} + \|\mathcal{U}'(\psi)^{-1/2} \chi\|_{L^2(\Omega)} \|\mathcal{U}'(\psi)^{1/2} \delta_h\|_{L^2(\Omega)} + \|\nabla \phi\|_{L^2(\Omega)} \|\delta_h\|_{H^1(\mathcal{T}_h)^*}.$$

Proceeding, we obtain a bound on  $\|\delta_h\|_{H^1(\mathcal{T}_h)^*}$ . Recall the definition of the  $L^2$  projection (32) and that we can bound

$$(111) \quad \|\delta_h\|_{H^1(\mathcal{T}_h)^*} = \sup_{w \in H^1(\mathcal{T}_h)} \frac{(\delta_h, w)}{\|w\|_{\text{DG}}} = \sup_{w \in H^1(\mathcal{T}_h)} \frac{(\delta_h, \Pi_h w)}{\|w\|_{\text{DG}}} \lesssim \sup_{w \in H^1(\mathcal{T}_h)} \frac{(\delta_h, \Pi_h w)}{\|\Pi_h w\|_{\text{DG}}}.$$



Define  $\hat{w}_h \in M_{h,0}^P$  as follows

$$(112) \quad \hat{w}_h = \begin{cases} \frac{1}{2}(\Pi_h w|_{T_E^1} + \Pi_h w|_{T_E^2}) & E \in \mathcal{E}_h^0 \quad E = \partial T_E^1 \cap \partial T_E^2, \\ 0 & E \subset \partial\Omega. \end{cases}$$

It is then easy to see that

$$\|(\mathbf{0}, \Pi_h w, \hat{w}_h)\| \lesssim \|\Pi_h w\|_{\text{DG}}.$$

Testing (108a) with  $(\mathbf{0}, \Pi_h w, \hat{w}_h)$  yields

$$(113) \quad \begin{aligned} (\delta_h, \Pi_h w) &= (\tilde{f}, \Pi_h w) - \alpha \mathcal{A}_h((\mathbf{q}_h, u_h, \hat{u}_h), (\mathbf{0}, \Pi_h w, \hat{w}_h)) \\ &\lesssim \|\tilde{f}\|_{H^1(\mathcal{T}_h)^*} \|\Pi_h w\|_{\text{DG}} + \alpha \|(\mathbf{q}_h, u_h, \hat{u}_h)\| \|(\mathbf{0}, \Pi_h w, \hat{w}_h)\|, \end{aligned}$$

where we used continuity of the form  $\mathcal{A}_h$  on the discrete spaces, see (58). This implies that

$$(114) \quad \|\delta_h\|_{H^1(\mathcal{T}_h)^*} \lesssim \|\tilde{f}\|_{H^1(\mathcal{T}_h)^*} + \alpha \|(\mathbf{q}_h, u_h, \hat{u}_h)\|.$$

We use the above in (110) and that  $\|u_h\|_{\text{DG}} \lesssim \|(\mathbf{q}_h, u_h, \hat{u}_h)\|$  which follows from (54). Applications of Young's inequality yield the result.  $\square$

**Remark 6.** *In the linearized subproblems arising from Newton's method, the function  $\chi = \mathcal{U}(\psi)$ . Thus, if  $\|\mathcal{U}'(\psi)^{-1/2}\mathcal{U}(\psi)\|_{L^\infty(\Omega)}$  is bounded uniformly as  $\text{ess inf } \psi \rightarrow -\infty$  or as  $\text{ess sup } \psi \rightarrow \infty$ , then one obtains a uniform estimate for the first two terms in (109). This is the case for the unilateral obstacle problems and examples (8a) and (8b) with  $\text{ess inf } \psi \rightarrow -\infty$ . For the double obstacle problem, the situation is more delicate. In the error analysis below, we obtain bounds in the first two norms of (109) that are uniformly bounded with  $\psi$  for  $\mathcal{U}$  given in (7a)–(7b).*

**6.2. Error Analysis.** In this subsection, we show error estimates between the discretized solutions of the linear subproblems (108) and their continuous counterparts resulting from applying Newton's method to the nonlinear subproblems (6): Find  $(u, \delta) \in H_0^1(\Omega) \times L^2(\Omega)$  such that

$$(115a) \quad \alpha(A\nabla u, \nabla v) + (\delta, v) = (\tilde{f}, v) \quad \forall v \in H_0^1(\Omega),$$

$$(115b) \quad (u, q) - (\mathcal{U}'(\psi)\delta, q) = (\phi + \chi, q) \quad \forall q \in L^2(\Omega).$$

The well-posedness of (115) follows from an immediate application of the Lax–Milgram Theorem since  $\mathcal{U}'(\psi) > 0$  a.e. in  $\Omega$ . See [46, Appendix B] for a similar argument.

Since we are interested in anisotropic diffusion, one can not assume  $H^{3/2+\eta}$ -regularity for  $\eta > 0$  for the solution  $u$  of the linearized subproblems (115). However, this regularity is needed for strong notions of consistency. In particular, it is required in order to use  $(-A\nabla u, u, \hat{u})$  as the first argument in the form  $\mathcal{A}_h$ , as is done in [24]. This is due to the presence of the normal flux on element boundaries in the form  $\mathcal{B}_h$ .

Here, we use the tools developed in [29] to define a suitable extension of the form  $\mathcal{A}_h$  that it is well defined for the following space. For  $s \in (0, 1/2)$ ,

$$(116) \quad V^s = \{u \in H^{1+s}(\Omega) : \nabla \cdot (A\nabla u) \in L^2(\Omega)\}.$$

First, we define the normal trace of the flux by duality. This requires the definition of the *face-to-element lifting* [29, Lemma 3.1]. Let  $\rho = 2d/(d - 2s)$ ,  $\rho'$  be its conjugate ( $1/\rho + 1/\rho' = 1$ ),

and let  $\gamma_{\partial T}$  denote the Dirichlet trace operator. For any  $E \subset \partial T$ , there exists a lifting operator:

$$(117) \quad L_E^T : W^{\frac{1}{\rho}, \rho'}(E) \rightarrow W^{1, \rho'}(T), \quad \gamma_{\partial T}(L_E^T(\varphi)) = \begin{cases} \varphi & \text{on } E, \\ 0 & \text{otherwise.} \end{cases}$$

With this map, the normal trace of a function belonging to the space

$$(118) \quad \mathbf{S}^d = \{\boldsymbol{\tau} \in L^\rho(\Omega) : \nabla_h \cdot \boldsymbol{\tau} \in L^2(T), \quad \forall T \in \mathcal{T}_h\}$$

is defined as a functional on  $W^{\frac{1}{\rho}, \rho'}(E)$  as follows

$$(119) \quad \langle (\boldsymbol{\tau} \cdot \mathbf{n}_K)|_E, \varphi \rangle_E = \int_T (\boldsymbol{\tau} \cdot \nabla L_E^T(\varphi) + (\nabla \cdot \boldsymbol{\tau}) L_E^T(\varphi)) \, dx.$$

Observe that the second term above is well-defined since  $W^{1, \rho'}(T) \hookrightarrow L^2(T)$  [25, Theorem 2.31]. Following [29, Section 4.5], we then define the form  $\eta_{\sharp} : \mathbf{S}^d \times V_h^p \times M_{h,0}^p \rightarrow \mathbb{R}$

$$(120) \quad \eta_{\sharp}(\boldsymbol{\tau}, (v_h, \hat{v}_h)) = \sum_{T \in \mathcal{T}_h} \sum_{E \in \mathcal{F}_T} \langle (\boldsymbol{\tau} \cdot \mathbf{n}_T)|_E, (v_h - \hat{v}_h)|_E \rangle_E,$$

where  $\mathcal{F}_T$  is the collection of all facets  $E$  of the element  $T$ . The above form allows us to define the following extension of  $\mathcal{A}_h$  given by  $\tilde{\mathcal{A}} : (\mathbf{S}^d \times H^1(\mathcal{T}_h) \times L^2(\mathcal{E}_h)) \times (\boldsymbol{\Sigma}_h^p \times V_h^p \times M_{h,0}^p) \rightarrow \mathbb{R}$

$$(121) \quad \tilde{\mathcal{A}}((\mathbf{q}, u, \hat{u}), (\mathbf{r}_h, v_h, \hat{v}_h)) = (A^{-1}\mathbf{q}, \mathbf{r}_h)_{\mathcal{T}_h} + \mathcal{B}_h(\mathbf{r}_h, (u, \hat{u})) \\ + \eta_{\sharp}(\mathbf{q}, (v_h, \hat{v}_h)) - (\mathbf{q}, \nabla_h v_h)_{\mathcal{T}_h}.$$

Finally, recall that  $\rho = 2d/(d - 2s)$  and equip the space  $\mathbf{S}^d$  with the following weighted norm

$$(122) \quad \|\boldsymbol{\tau}\|_{\mathbf{S}^d}^2 = \sum_{T \in \mathcal{T}_h} \left( h_T^{2s} \|A^{-1/2}\boldsymbol{\tau}\|_{L^\rho(T)}^2 + h_T^2 \|A^{-1/2}\nabla \cdot \boldsymbol{\tau}\|_{L^2(T)}^2 \right).$$

**Lemma 6.2** (Consistency). *Let  $u \in V^s \cap H_0^1(\Omega)$  and  $\delta \in L^2(\Omega)$  be the solutions of the linearized sub-problem (115). Denote by  $\boldsymbol{\sigma}(u) = -A\nabla u$ . Then,*

$$(123a) \quad \alpha \tilde{\mathcal{A}}((\boldsymbol{\sigma}(u), u, u), (\mathbf{r}_h, v_h, \hat{v}_h)) + (\delta, v_h) = (\tilde{f}, v_h)$$

$$(123b) \quad (u, q_h) - (\mathcal{U}'(\psi)\delta, q_h) = (\phi + \chi, q_h),$$

for all  $(\mathbf{r}_h, v_h, \hat{v}_h) \in \boldsymbol{\Sigma}_h^p \times V_h^p \times M_{h,0}^k$  and for all  $q_h \in V_h^p$ .

*Proof.* We first check that  $(\boldsymbol{\sigma}(u), u, u) \in \mathbf{S}^d \times H^1(\mathcal{T}_h) \times L^2(\mathcal{E}_h)$ . To this end, observe that if  $u \in V^s$  then  $\nabla u \in H^s(T)^d$  for any element  $T \in \mathcal{T}_h$ . Then, by the Sobolev embedding theorem [25, Theorem 2.31] and the assumption that  $A \in L^\infty(\Omega)$ , we have that  $A\nabla u \in L^\rho(T)$  where  $\rho = 2d/(d - 2s)$  for any  $T \in \mathcal{T}_h$ . From trace theory, it also follows that  $u \in L^2(\mathcal{E}_h)$ .

To show the consistency property, we use [29, Lemma 4.16] to obtain that

$$(124) \quad \eta_{\sharp}(\boldsymbol{\sigma}(u), (v_h, \hat{v}_h)) - (\boldsymbol{\sigma}(u), \nabla_h v_h)_{\mathcal{T}_h} = (\nabla \cdot \boldsymbol{\sigma}(u), v_h)_{\mathcal{T}_h}.$$

Further, observe that by definition

$$\mathcal{B}_h(\mathbf{r}_h, u, u) = (\mathbf{r}_h, \nabla u)_{\mathcal{T}_h} = -(A^{-1}\boldsymbol{\sigma}(u), \mathbf{r}_h)_{\mathcal{T}_h}.$$

Collecting the above and using that  $\alpha \nabla \cdot \boldsymbol{\sigma}(u) = \tilde{f} - \delta \in L^2(\Omega)$  yield (123a). The derivation of (123b) is immediate since  $V_h^p \subset L^2(\Omega)$ .  $\square$

The next Lemma shows that the form  $\mathcal{A}$  indeed defines an extension of  $\mathcal{A}_h$ .

**Lemma 6.3** (Extension). *For  $\mathbf{q}_h \in \Sigma_h^p$ , we have that*

$$(125) \quad \mathcal{B}_h(\mathbf{q}_h, (v_h, \hat{v}_h)) = -\eta_{\sharp}(\mathbf{q}_h, (v_h, \hat{v}_h)) + (\mathbf{q}_h, \nabla_h v_h)_{\mathcal{T}_h} \quad \forall (v_h, \hat{v}_h) \in V_h^p \times M_h^p.$$

*Proof.* Fix  $T \in \mathcal{T}_h$  and let  $E \in \mathcal{F}_T$ . By definition of the duality pairing (119) and Green's theorem since  $\mathbf{q}_h|_T$  is smooth, we write

$$\begin{aligned} \langle (\mathbf{q}_h \cdot \mathbf{n}_T)|_E, (v_h - \hat{v}_h)|_E \rangle &= \int_T (\mathbf{q}_h \cdot \nabla L_E^T(v_h - \hat{v}_h) + (\nabla \cdot \mathbf{q}_h) L_E^T(v_h - \hat{v}_h)) \, dx \\ &= \int_{\partial T} \mathbf{q}_h \cdot \mathbf{n}_T L_E^T(v_h - \hat{v}_h) \, ds \\ &= \int_E \mathbf{q}_h \cdot \mathbf{n}_T (v_h - \hat{v}_h) \, ds. \end{aligned}$$

The last equality holds since  $L_E^T(v_h - \hat{v}_h)$  vanishes on  $\partial T \setminus E$ . Summing over all  $E \in \mathcal{F}_T$  and over all  $T \in \mathcal{T}_h$  yields the result.  $\square$

Proceeding, we derive error equations. Observe that there is no Galerkin orthogonality property here. However, the previous results allow us to adopt an argument similar to Strang's Second Lemma.

**Lemma 6.4** (Error equations). *Let  $(\mathbf{q}_h, u_h, \hat{u}_h) \in \Sigma_h^p \times V_h^p \times M_{h,0}^p$  and  $\delta_h \in V_h^p$  solve (107). For any  $(\mathbf{r}_h, v_h, \hat{v}_h) \in \Sigma_h^p \times V_h^p \times M_{h,0}^p$  and  $\varphi_h \in V_h^p$ , let  $(\mathbf{e}_h, e_h, \hat{e}_h) = (\mathbf{q}_h - \mathbf{r}_h, u_h - v_h, \hat{u}_h - \hat{v}_h)$  and  $e_{\delta,h} = \delta_h - \varphi_h$ .*

*The following error equations hold for all  $(\mathbf{w}_h, w_h, \hat{w}_h) \in \Sigma_h^p \times V_h^p \times M_{h,0}^p$  and for all  $q_h \in V_h^p$ ,*

$$(126) \quad \alpha \mathcal{A}_h((\mathbf{e}_h, e_h, \hat{e}_h), (\mathbf{w}_h, w_h, \hat{w}_h)) + (e_{\delta,h}, w_h) = \mathcal{L}_1(\mathbf{w}_h, w_h, \hat{w}_h),$$

$$(127) \quad (e_h, q_h) - (\mathcal{U}'(\psi) e_{\delta,h}, q_h) = \mathcal{L}_2(q_h),$$

where  $\mathcal{L}_1$  and  $\mathcal{L}_2$  are given by

$$(128) \quad \begin{aligned} \mathcal{L}_1(\mathbf{w}_h, w_h, \hat{w}_h) &= (\delta - \varphi_h, w_h) \\ &\quad + \alpha \tilde{\mathcal{A}}((\boldsymbol{\sigma}(u), u, u), (\mathbf{w}_h, w_h, \hat{w}_h)) - \alpha \mathcal{A}_h((\mathbf{r}_h, v_h, \hat{v}_h), (\mathbf{w}_h, w_h, \hat{w}_h)) \end{aligned}$$

$$(129) \quad \mathcal{L}_2(q_h) = (u - v_h, q_h) - (\mathcal{U}'(\psi)(\delta - \varphi_h), q_h).$$

*Proof.* Since  $(\mathbf{q}_h, u_h, \hat{u}_h)$  solve (108a)-(108b) and by linearity of  $\mathcal{A}_h$ , we have

$$(130) \quad \alpha \mathcal{A}_h((\mathbf{e}_h, e_h, \hat{e}_h), (\mathbf{w}_h, w_h, \hat{w}_h)) = (\tilde{f}, w_h) - (\delta_h, w_h) - \alpha \mathcal{A}_h((\mathbf{r}_h, v_h, \hat{v}_h), (\mathbf{w}_h, w_h, \hat{w}_h)).$$

With the consistency property Lemma 6.2,

$$(131) \quad \begin{aligned} \alpha \mathcal{A}_h((\mathbf{e}_h, e_h, \hat{e}_h), (\mathbf{w}_h, w_h, \hat{w}_h)) &= (\delta - \delta_h, w_h) \\ &\quad + \alpha \tilde{\mathcal{A}}((\boldsymbol{\sigma}(u), u, u), (\mathbf{w}_h, w_h, \hat{w}_h)) - \alpha \mathcal{A}_h((\mathbf{r}_h, v_h, \hat{v}_h), (\mathbf{w}_h, w_h, \hat{w}_h)). \end{aligned}$$

With writing  $\delta - \delta_h = \delta - \varphi_h - e_{\delta,h}$ , we obtain (126). The equality given by (127) is immediate.  $\square$

**Theorem 6.5** (Convergence). *Let  $(\mathbf{q}_h, u_h, \hat{u}_h)$  solve (108) and let  $u$  solve the linearized sub-problem (115). Assume that  $u \in V^s$  and let  $\boldsymbol{\sigma}(u) = -A\nabla u$ . The following estimate holds*

$$(132) \quad \|\boldsymbol{\sigma}(u) - \mathbf{q}_h, u - u_h, \hat{u} - \hat{u}_h\| + \|\delta - \delta_h\|_{H^1(\mathcal{T}_h)^*} \lesssim \mathcal{E}(u) + \mathcal{E}(\delta),$$

where  $\mathcal{E}(u)$  and  $\mathcal{E}(\delta)$  are best approximation errors given by

$$(133) \quad \mathcal{E}(u) = \inf_{(\mathbf{r}_h, v_h, \hat{v}_h)} (\|u - v_h\|_{\text{DG}} + \|\boldsymbol{\sigma}(u) - \mathbf{r}_h\|_{\mathcal{S}^d} + \|(\boldsymbol{\sigma}(u) - \mathbf{r}_h, u - v_h, u - \hat{v}_h)\|)$$

$$(134) \quad \mathcal{E}(\delta) = \inf_{\varphi_h} (\|\delta - \varphi_h\|_{H^1(\mathcal{T}_h)^*} + \|\mathcal{U}'(\psi)\|_{L^\infty(\Omega)}^{1/2} \|\delta - \varphi_h\|_{L^2(\Omega)}).$$

The hidden constant in (132) is independent of  $\psi$ .

Error estimates are shown in the following corollary; see Appendix B for the proof.

**Corollary 2.** *Assume that  $u \in V^s$  and  $\delta \in H^s(\Omega)$  for  $s \in (0, 1/2)$ , then*

$$(135) \quad \begin{aligned} & \|(\boldsymbol{\sigma}(u) - \mathbf{q}_h, u - u_h, u - \hat{u}_h)\| + \|\delta - \delta_h\|_{H^1(\mathcal{T}_h)^*} \\ & \lesssim h^s (\|u\|_{H^{1+s}(\Omega)} + \|\mathcal{U}'(\psi)\|_{L^\infty(\Omega)}^{1/2} \|\delta\|_{H^s(\Omega)}) \\ & + h (\|\nabla \cdot \boldsymbol{\sigma}(u)\|_{L^2(\Omega)} + \|\delta\|_{L^2(\Omega)}). \end{aligned}$$

**Remark 7.** *If the solution has additional regularity  $u \in H^{p+1}(\Omega)$  and  $\delta \in H^{p-1}(\Omega)$  for  $p \geq 1$ , then optimal error estimates can be readily derived. One can also easily obtain an error estimate for  $\|\mathcal{U}'(\psi)^{1/2}(\delta - \delta_h)\|_{L^2(\Omega)}$ . However, the corresponding bound degenerates with  $\psi \rightarrow -\infty$  or with  $\psi \rightarrow \infty$ . In contrast, observe that the bound (135) remains bounded.*

*Proof.* (Theorem 6.5) **Step 1.** (Estimating the consistency error  $\mathcal{L}_1(\mathbf{w}_h, w_h, \hat{w}_h)$  for any  $(\mathbf{w}_h, w_h, \hat{w}_h) \in \boldsymbol{\Sigma}_h^p \times V_h^p \times M_{h,0}^p$ ). Recalling the definition of  $\mathcal{L}_1$  in (128), we bound its first term by the definition of  $\|\cdot\|_{H^1(\mathcal{T}_h)^*}$  and by (54).

$$(136) \quad |(\delta - \varphi_h, w_h)| \leq \|\delta - \varphi_h\|_{H^1(\mathcal{T}_h)^*} \|w_h\|_{\text{DG}} \lesssim \|\delta - \varphi_h\|_{H^1(\mathcal{T}_h)^*} \|(\mathbf{w}_h, w_h, \hat{w}_h)\|.$$

Consider the last two terms in (128) which we denote by  $\alpha Q$ . With Lemma 6.3, we write

$$(137) \quad \begin{aligned} Q &= (A^{-1}(\boldsymbol{\sigma}(u) - \mathbf{r}_h), \mathbf{w}_h)_{\mathcal{T}_h} + \mathcal{B}_h(\mathbf{w}_h, u - v_h, u - \hat{v}_h) \\ &+ \eta_{\sharp}(\boldsymbol{\sigma}(u) - \mathbf{r}_h, w_h, \hat{w}_h) - (\boldsymbol{\sigma}(u) - \mathbf{r}_h, \nabla_h w_h) = Q_1 + \dots + Q_4. \end{aligned}$$

From Cauchy-Schwarz inequality and the definition of  $\|\cdot\|$  (53), it is easy to see that

$$(138) \quad \begin{aligned} Q_1 + Q_4 &\leq \|A^{-1/2}(\boldsymbol{\sigma}(u) - \mathbf{r}_h)\|_{L^2(\Omega)} (\|A^{-1/2}\mathbf{w}_h\|_{L^2(\Omega)} + \|A^{1/2}\nabla_h w_h\|_{L^2(\Omega)}) \\ &\lesssim \|A^{-1/2}(\boldsymbol{\sigma}(u) - \mathbf{r}_h)\|_{L^2(\Omega)} \|(\mathbf{w}_h, w_h, \hat{w}_h)\|. \end{aligned}$$

For  $Q_2$ , an application of trace inequality shows that

$$(139) \quad \begin{aligned} Q_2 &\lesssim \|A^{-1/2}\mathbf{w}_h\|_{\mathcal{T}_h} \|A^{1/2}\nabla_h(u - v_h)\|_{\mathcal{T}_h} \\ &+ \left( \sum_{E \in \mathcal{E}_h} h_E^{-1} \|u - v_h - (u - \hat{v}_h)\|_{L^2(E)}^2 \right)^{1/2} \|A^{-1/2}\mathbf{w}_h\|_{L^2(\Omega)}. \end{aligned}$$

We utilize [29, Lemma 3.2] (with  $p = \rho$  and  $q = 2$ ) to bound  $Q_3$ . In particular, we have that

$$(140) \quad \begin{aligned} & \langle ((\boldsymbol{\sigma}(u) - \mathbf{r}_h) \cdot \mathbf{n}_T)|_E, (w_h - \hat{w}_h)|_E) \rangle_E \\ & \lesssim (h_T^s \|A^{-1/2}(\boldsymbol{\sigma}(u) - \mathbf{r}_h)\|_{L^\rho(T)} + h_T \|A^{-1/2}(\nabla \cdot (\boldsymbol{\sigma}(u) - \mathbf{r}_h))\|_{L^2(T)}) h_E^{-1/2} \|w_h - \hat{w}_h\|_{L^2(E)}. \end{aligned}$$

Summing over all  $E \in \mathcal{F}_T$  and over all  $T \in \mathcal{T}_h$ , recalling the definition of  $\|\cdot\|_{\mathcal{S}^d}$  (122) and applying Cauchy-Schwarz inequality for sums, we obtain

$$(141) \quad Q_3 \lesssim \|\boldsymbol{\sigma}(u) - \mathbf{r}_h\|_{\mathcal{S}^d} \|(\mathbf{w}_h, w_h, \hat{w}_h)\|.$$

Collecting the estimates above, we conclude that

$$(142) \quad \sup_{(\mathbf{w}_h, w_h, \hat{w}_h)} \frac{|\mathcal{L}_1(\mathbf{w}_h, w_h, \hat{w}_h)|}{\|(\mathbf{w}_h, w_h, \hat{w}_h)\|} \lesssim \|\delta - \varphi_h\|_{H^1(\mathcal{T}_h)^*} + \|\boldsymbol{\sigma}(u) - \mathbf{r}_h\|_{\mathbf{S}^d} + \|(\boldsymbol{\sigma}(u) - \mathbf{r}_h, u - v_h, u - \hat{v}_h)\|.$$

**Step 2.** (Bounding the dual norm of  $e_{\delta,h}$ ). With similar arguments to (111), observe that

$$(143) \quad \|e_{\delta,h}\|_{H^1(\mathcal{T}_h)^*} \lesssim \sup_{w \in H^1(\mathcal{T}_h)} \frac{|(e_{\delta,h}, \Pi_h w)|}{\|\Pi_h w\|_{\text{DG}}}.$$

Testing (126) with  $(\mathbf{0}, \Pi_h w, \hat{w}_h)$ , with  $\hat{w}_h$  defined in (112), we write

$$(144) \quad (e_{\delta,h}, \Pi_h w) = \mathcal{L}_1(\mathbf{0}, w_h, \hat{w}_h) - \alpha \mathcal{A}_h((\mathbf{e}_h, e_h, \hat{e}_h), (\mathbf{0}, w_h, \hat{w}_h)).$$

From (142), continuity of  $\mathcal{A}_h$ , and that  $\|(\mathbf{0}, \Pi_h w, \hat{w}_h)\| \lesssim \|\Pi_h w\|_{\text{DG}}$ , we obtain that

$$(145) \quad \|e_{\delta,h}\|_{H^1(\mathcal{T}_h)^*} \lesssim \sup_{(\mathbf{w}_h, w_h, \hat{w}_h)} \frac{\mathcal{L}_1(\mathbf{w}_h, w_h, \hat{w}_h)}{\|(\mathbf{w}_h, w_h, \hat{w}_h)\|} + \|(\mathbf{e}_h, e_h, \hat{e}_h)\|.$$

**Step 3.** (Bounding  $\|(\mathbf{e}_h, e_h, \hat{e}_h)\|$ ). We split the error into  $(\mathbf{e}_h, e_h, \hat{e}_h) = (\boldsymbol{\eta}_h, \eta_h, \hat{\eta}_h) + (\boldsymbol{\rho}_h, \rho_h, \hat{\rho}_h)$  and  $e_{\delta,h} = \eta_{\delta,h} + \rho_{\delta,h}$  where  $(\boldsymbol{\eta}_h, \eta_h, \hat{\eta}_h, \eta_{\delta,h})$  solves (126)-(127) with  $\mathcal{L}_2 = 0$  and  $(\boldsymbol{\rho}_h, \rho_h, \hat{\rho}_h, \rho_{\delta,h})$  solves (126)-(127) with  $\mathcal{L}_1 = 0$ . The existence of such a decomposition follows by the well-posedness of the formulation and the fact that  $\mathcal{L}_1$  and  $\mathcal{L}_2$  are bounded linear functionals on  $\boldsymbol{\Sigma}_h^p \times V_h^p \times M_{h,0}^p$ .

*Step 3.1.* We begin with bounding  $\|(\boldsymbol{\eta}_h, \eta_h, \hat{\eta}_h)\|$ . From Lemma 4.4, we obtain

$$(146) \quad \|(\boldsymbol{\eta}_h, \eta_h, \hat{\eta}_h)\|^2 \lesssim \mathcal{A}_h((\boldsymbol{\eta}_h, \eta_h, \hat{\eta}_h), (\mathbf{r}_h, \eta_h, \hat{\eta}_h)).$$

Since  $(\boldsymbol{\eta}_h, \eta_h, \hat{\eta}_h)$  solve (126), we have

$$(147) \quad \alpha \mathcal{A}_h((\boldsymbol{\eta}_h, \eta_h, \hat{\eta}_h), (\mathbf{r}_h, \eta_h, \hat{\eta}_h)) = -(\eta_{\delta,h}, \eta_h) + \mathcal{L}_1(\mathbf{w}_h, \eta_h, \hat{\eta}_h).$$

Testing (127) with  $\eta_{\delta,h}$  and recalling that  $\mathcal{L}_2 = 0$  yield

$$(148) \quad \alpha \mathcal{A}_h((\boldsymbol{\eta}_h, \eta_h, \hat{\eta}_h), (\mathbf{r}_h, \eta_h, \hat{\eta}_h)) = -(\mathcal{U}'(\psi)\eta_{\delta,h}, \eta_{\delta,h}) + \mathcal{L}_1(\mathbf{r}_h, \eta_h, \hat{\eta}_h) \leq \mathcal{L}_1(\mathbf{r}_h, \eta_h, \hat{\eta}_h).$$

Invoking (142), we obtain

$$(149) \quad \|(\boldsymbol{\eta}_h, \eta_h, \hat{\eta}_h)\| \lesssim \|\delta - \varphi\|_{H^1(\mathcal{T}_h)^*} + \|\boldsymbol{\sigma}(u) - \mathbf{r}_h\|_{\mathbf{S}^d} + \|(\boldsymbol{\sigma}(u) - \mathbf{r}_h, u - v_h, u - \hat{v}_h)\|.$$

*Step 3.2.* To bound  $\|(\boldsymbol{\rho}_h, \rho_h, \hat{\rho}_h)\|$ , we use that  $(\boldsymbol{\rho}_h, \rho_h, \hat{\rho}_h, \rho_{\delta,h})$  solves (126)-(127) with  $\mathcal{L}_1 = 0$ . Namely, we can write for any  $\mathbf{w}_h \in \boldsymbol{\Sigma}_h^p$

$$(150) \quad \begin{aligned} \mathcal{A}_h((\boldsymbol{\rho}_h, \rho_h, \hat{\rho}_h), (\mathbf{w}_h, \rho_h, \hat{\rho}_h)) &= -(\rho_{\delta,h}, \rho_h) \\ &= -\mathcal{L}_2(\rho_{\delta,h}) - (\mathcal{U}'(\psi)\rho_{\delta,h}, \rho_{\delta,h}). \end{aligned}$$

That is, we derived that

$$(151) \quad \mathcal{A}_h((\boldsymbol{\rho}_h, \rho_h, \hat{\rho}_h), (\mathbf{w}_h, \rho_h, \hat{\rho}_h)) + (\mathcal{U}'(\psi)\rho_{\delta,h}, \rho_{\delta,h}) = -\mathcal{L}_2(\rho_{\delta,h}).$$

With applications of Hölder's and Poincaré's inequality along with (54), we estimate

$$(152) \quad |\mathcal{L}_2(\rho_{\delta,h})| \lesssim \|u - v_h\|_{\text{DG}} \|\rho_{\delta,h}\|_{H^1(\mathcal{T}_h)^*} + \|\mathcal{U}'(\psi)^{1/2}(\delta - \varphi_h)\|_{L^2(\Omega)} \|\mathcal{U}'(\psi)^{1/2}\rho_{\delta,h}\|_{L^2(\Omega)}.$$

From (145) with  $\mathcal{L}_1 = 0$ , we have that

$$(153) \quad \|\rho_{\delta,h}\|_{H^1(\mathcal{T}_h)^*} \leq \|(\boldsymbol{\rho}_h, \rho_h, \hat{\rho}_h)\|.$$

Along with Lemma 4.4 and (151), this allows us to bound

$$(154) \quad \|(\boldsymbol{\rho}_h, \rho_h, \hat{\rho}_h)\| + \|\mathcal{U}'(\psi)^{1/2} \rho_{\delta,h}\|_{L^2(\Omega)} \lesssim \|u - v_h\|_{\text{DG}} + \|\mathcal{U}'(\psi)^{1/2}(\delta - \varphi_h)\|_{L^2(\Omega)}.$$

The final result is concluded by combining (145) with (149) and (154) along with applications of the triangle inequality.  $\square$

## 7. NUMERICAL RESULTS

In this section, we consider anisotropic diffusion and obstacle examples. We implement Algorithm 3 and denote the converged solution by  $(u_h, \mathbf{q}_h, \hat{u}_h) \in \boldsymbol{\Sigma}_h^p \times V_h^p \times M_{h,g}^p$ . The stopping criteria is  $\|u_h^k - u_h^{k-1}\|_{L^2(\Omega)} < \text{tol}$ . All simulation results were obtained using the NGSolve software [59]. We share our code at <https://github.com/ramimasri/FOSPG-first-order-system-proximal-Galerkin.git>.

**7.1. Anisotropic diffusion.** We consider three benchmark examples taken from [40, 52]. While the standard hybrid mixed method [7] may violate the discrete maximum principle, the FOSPG produces a solution  $\mathcal{U}(\psi_h)$  satisfying the pointwise bounds everywhere. Figure 2 shows the converged solutions  $\mathcal{U}(\psi_h)$  for  $p = 2$ .

**Example 7.1** (Oblique flow). We adapt this example from [40]. Consider  $\Omega = (0, 1)^2$  and

$$A = Q \begin{pmatrix} 1 & 0 \\ 0 & \lambda \end{pmatrix} Q^T, \quad Q = \begin{pmatrix} \cos(\theta) & -\sin(\theta) \\ \sin(\theta) & \cos(\theta) \end{pmatrix},$$

where  $\lambda = 10^{-3}$  and  $\theta = 2\pi/9$ . We let  $f = 0$  and

$$g(x, 0) = \begin{cases} 1 & \text{if } x \leq 0.2 \\ 2 - 5x & \text{if } 0.2 < x \leq 0.3, \\ 0.5 & \text{if } x > 0.3, \end{cases} \quad g(x, 1) = \begin{cases} 0.5 & \text{if } x \leq 0.7, \\ 4 - 5x & \text{if } 0.7 < x \leq 0.8, \\ 0 & \text{if } x > 0.8. \end{cases}$$

Further, we set  $g(0, y) = g(y, 0)$  and  $g(1, y) = g(y, 1)$ .

**Example 7.2** (Vertical faults). We consider the example from [40] and consider  $\Omega = \Omega_1 \cup \Omega_2$  with  $\Omega_2 = \Omega \setminus \Omega_1$ ,  $\Omega_1 = \Omega_1^\ell \cup \Omega_1^r$  where

$$\Omega_1^\ell = (0, 0.5) \times \bigcup_{k=0}^4 [0.05 + 0.2k, 0.15 + 0.2k], \quad \Omega_1^r = (0.5, 1) \times \bigcup_{k=0}^4 [0.2k, 0.2k + 0.1].$$

We set

$$A|_{\Omega_1} = \begin{pmatrix} 10^3 & 0 \\ 0 & 10 \end{pmatrix}, \quad A|_{\Omega_2} = \begin{pmatrix} 10^{-2} & 0 \\ 0 & 10^{-3} \end{pmatrix},$$

the source term  $f = 0$ , and the boundary data  $g(x, y) = 1 - x$ .

**Example 7.3** (Punctured domain). We adapt the example from [52]. The domain  $\Omega = \Omega_0 \setminus \Omega_1 = (0, 1)^2 \setminus (4/9, 5/9)^2$ . We let

$$A = Q \begin{pmatrix} \lambda & 0 \\ 0 & 1 \end{pmatrix} Q^T, \quad Q = \begin{pmatrix} \cos(\theta) & -\sin(\theta) \\ \sin(\theta) & \cos(\theta) \end{pmatrix},$$

where  $\lambda = 10^3$  and  $\theta = \pi \sin(x) \sin(y)$ . We set  $f = 0$ ,  $u|_{\partial\Omega_1} = 1$ , and  $u|_{\partial\Omega_2} = 0$ .

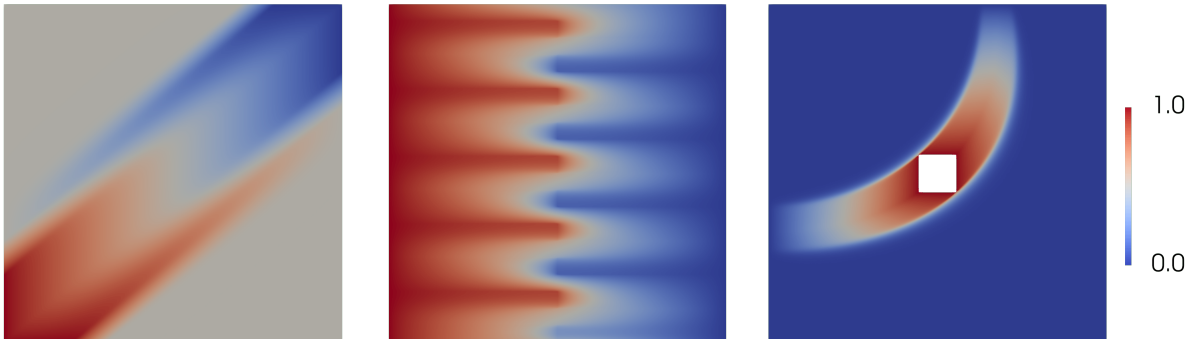


FIGURE 2. Computed solution  $\mathcal{U}(\psi_h)$  for the oblique flow Example 7.1 (left), for the vertical faults Example 7.2 (middle) and for the punctured domain Example 7.3 (right). We set  $p = 2$ ,  $h \approx 0.006$ ,  $\text{tol} = 1e - 10$ , and select the superposition operator  $\mathcal{U}$  given in (7b). The solutions  $\mathcal{U}(\psi_h)$  satisfy the discrete maximum principle by design. Further, the obtained flux approximation  $\mathbf{q}_h$  retains the local mass conservation property. In particular,  $\max_{T \in \mathcal{T}_h} |(\nabla \cdot \mathbf{q}_h - f, 1)_T| < 5 \cdot 10^{-13}$  for all three examples. For Example 7.1 and Example 7.2, we set  $\alpha^k = 4^k$  and  $\mathcal{S}(\psi_h^k) = 0$ . For Example 7.3, we set  $\alpha^0 = 10^{-4}$ ,  $\alpha^k = 1.5\alpha^{k-1}$ , and use  $\mathcal{S}(\psi_h^k)$  given in (155) with  $\epsilon_1 = \epsilon_2 = 0.1$ .

We found Example 7.3 to be the most challenging, inspiring us to explore this example further. In particular, we consider the following choice for  $\mathcal{S}(\psi_h^k)$  in (59c):

$$(155) \quad (\mathcal{S}(\psi_h^k), q_h) = \epsilon_1 h^{p+1} (\psi_h^k, q_h) + \epsilon_2 h^{p+1} (\nabla_h \psi_h^k, \nabla_h q_h) \quad \forall q_h \in V_h^p,$$

where  $\epsilon_1, \epsilon_2 \geq 0$ . This choice provided additional control on the broken  $H^1$  norm of  $\psi_h^k$  leading to a stable solution  $\mathcal{U}(\psi_h)$ . For  $p = 0, 1$ , such stabilization is not needed; see Remark 8. For  $p = 1$ , we use a quadrature rule of order 2 that includes the element vertices for a more stable solution  $\mathcal{U}(\psi_h)$  in all of this section. We remark that the choice of stabilization whether via special quadrature rules or additional terms like in (155) requires a detailed and additional study.

Figure 3 compares the standard mixed method solution  $u_h^{\text{mixed}}$  [24] to the solutions  $(u_h, \mathcal{U}(\psi_h))$  generated by Algorithm 3. We observe that  $u_h^{\text{mixed}}$  violates DMP even with fine meshes for  $p = 0$ . For  $p = 2$ , mesh refinement improves the solution; however,  $u_h^{\text{mixed}}$  is still not bound preserving. This is also evident from Table 1, which reports the minimum and maximum values of  $u_h^{\text{mixed}}$  and  $\mathcal{U}(\psi_h)$  over the quadrature points. The classical solution  $u_h^{\text{mixed}}$  violates the DMP while the solution  $\mathcal{U}(\psi_h)$  remains between 0 and 1 everywhere. Furthermore, the solution  $u_h$  has bound-preserving local averages, a property that can be optionally used in postprocessing to locally construct a bound-preserving  $\tilde{u}_h$  (see Remark 9).

**Remark 8** (Local mass conservation for anisotropic diffusion). *Corollary 1 guarantees mass-conservation at the elements where  $u_h^*$  is strictly within the bounds. Nonetheless, we numerically observe local mass conservation everywhere. Example 7.3 presented further challenges*

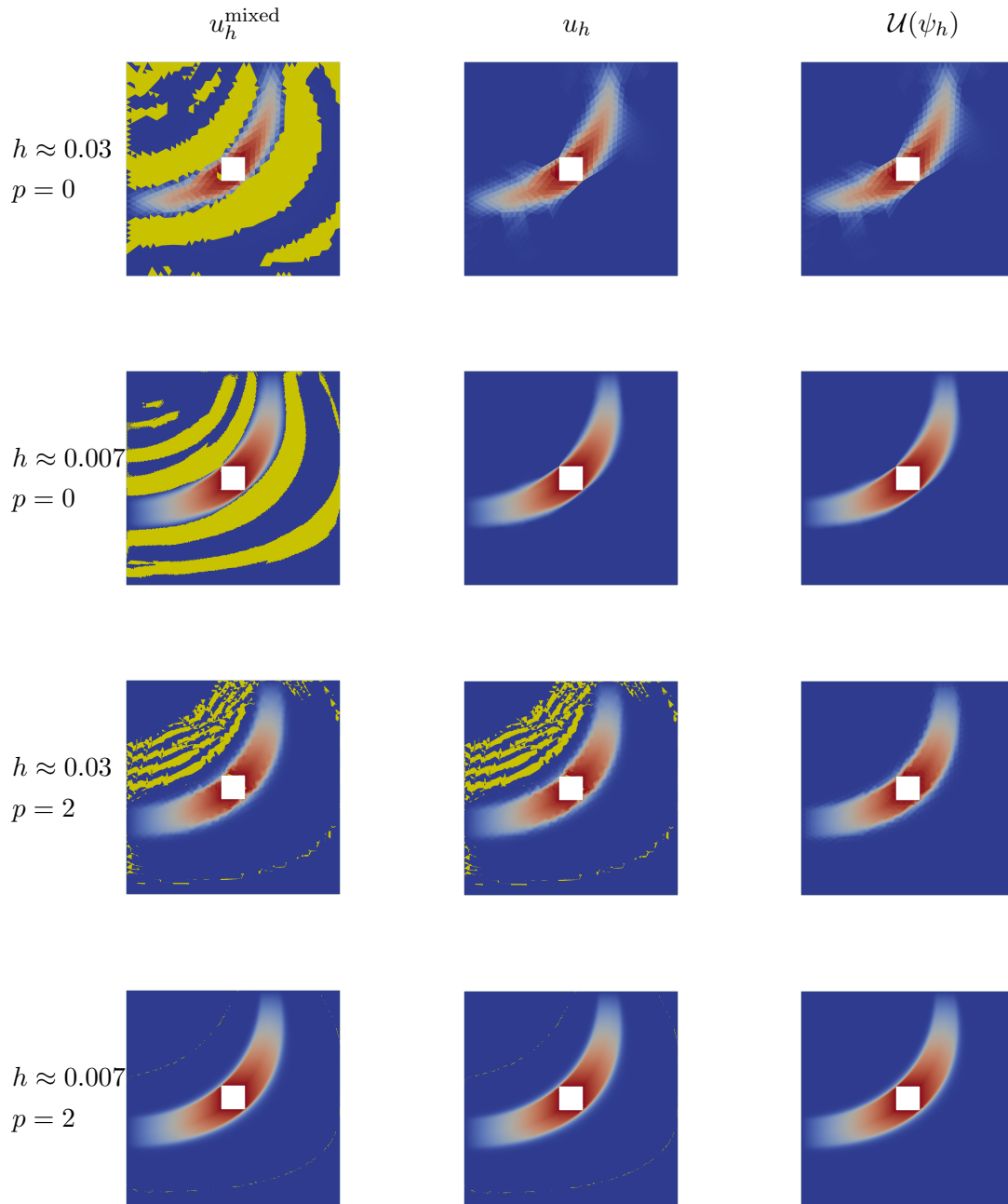


FIGURE 3. Comparison between the standard hybrid mixed solution  $u_h^{\text{mixed}}$  and the FOSPG solutions  $u_h$  and  $\mathcal{U}(\psi_h)$  of Algorithm 3 with  $\mathcal{U}$  given in (7b). We use (155) and set  $\epsilon_1 = \epsilon_2 = 0.0$  for  $p = 0$  and  $\epsilon_1 = \epsilon_2 = 0.1$  for  $p = 2$ . The violation of DMP is indicated with yellow.



	$h = 0.03$				$h = 0.007$			
$p$	$\max u_h^{\text{mixed}}$	$\min u_h^{\text{mixed}}$	$\max \mathcal{U}(\psi_h)$	$\min \mathcal{U}(\psi_h)$	$\max u_h^{\text{mixed}}$	$\min u_h^{\text{mixed}}$	$\max \mathcal{U}(\psi_h)$	$\min \mathcal{U}(\psi_h)$
0	1.014	-0.620	0.996	$2.78e - 06$	1.004	-0.191	0.997	$1.85e - 06$
1	1.144	-0.161	1.000	$6.91e - 08$	1.085	$-1.95e - 03$	1.000	$4.89e - 06$
2	1.157	-0.012	0.994	$3.10e - 07$	1.081	$-8.48e - 11$	0.999	$3.29e - 06$

TABLE 1. Minimum and maximum values (at quadrature points) of the standard mixed method solution  $u_h^{\text{mixed}}$  and the solution  $\mathcal{U}(\psi_h)$  obtained by Algorithm 3 (hybridized FOSPG) on Example 7.3. Both methods return a numerical flux that is locally mass conserving up to almost double precision-accuracy  $\mathcal{O}(10^{-12})$ . The solution  $\mathcal{U}(\psi_h)$ , with  $\mathcal{U}$  given by (7b), is bound preserving everywhere in the domain by construction. However, the mixed method solution  $u_h^{\text{mixed}}$  violates the DMP. Here, we use the stabilization term (155) with  $\epsilon_1 = \epsilon_2 = 0.1$  for each polynomial degree  $p$ .

and required  $\epsilon_1, \epsilon_2 \neq 0$  since the magnitude of the converged latent variable  $\psi_h^k$  is of the order  $\max |\psi_h^k| \approx 10^{10}$  otherwise. Having such a large solution variable can introduce round-off errors that dominate the discretization error in the computed solution. Including the term (155) with  $\epsilon_1 = \epsilon_2 = 0.1$  limited the magnitude of  $\psi_h^k$ , delivering local mass conservation up to almost double-precision accuracy; i.e.,  $\max_{T \in \mathcal{T}_h} |(\nabla \cdot \mathbf{q}_h - f, 1)_T| = \mathcal{O}(10^{-12})$ .

**Remark 9** (Post processing  $u_h$ ). Recall that the local average of the solution  $u_h$  is bound preserving by Remark 2. Therefore, we can apply the classical linear scaling limiter [64] to obtain a bound-preserving polynomial approximation over the whole domain. On each element  $T \in \mathcal{T}_h$ , let  $\bar{u}_h$  be the cell average of  $u_h$ ,  $M = \max_{x \in T} u_h(x)$  and  $m = \min_{x \in T} u_h(x)$ . Define  $\tilde{u}_h$  as

$$\tilde{u}_h(x) = \bar{u}_h + \theta(u_h(x) - \bar{u}_h), \quad \theta = \min \left\{ \left| \frac{\bar{u} - \bar{u}_h}{M - \bar{u}_h} \right|, \left| \frac{\underline{u} - \bar{u}_h}{m - \bar{u}_h} \right|, 1 \right\}, \quad x \in T.$$

Then  $\underline{u} \leq \tilde{u}_h(x) \leq \bar{u}$  for all  $x \in T$ . Figure 4 shows the solutions  $u_h$  and the limited solution  $\tilde{u}_h$ . It is clear that the limited solution is bound-preserving.

**7.2. Obstacle problems.** We consider two examples taken from [46]. The first one is a smooth biactive solution, see [46, Subsection 4.8.1] for a discussion on *biactivity* and the challenges this property presents to active set methods. The second example is a nonsmooth spherical obstacle problem.

**Example 7.4** (Biactive solution). In (4), we set  $\Omega = [-1, 1] \times [-1, 1]$ ,  $\underline{u} = 0$ , and  $\bar{u} = \infty$ . We consider the smooth manufactured solution  $u$  with source term  $f$  given by:

$$u(x, y) = \begin{cases} 0 & \text{if } x < 0, \\ x^4 & \text{otherwise,} \end{cases} \quad f(x, y) = \begin{cases} 0 & \text{if } x < 0, \\ -12x^2 & \text{otherwise.} \end{cases}$$

We set  $g = u|_{\partial\Omega}$ . Figure 5 demonstrates that the approximation resulting from Algorithm 3 yields the expected error rates for each  $p \in \{0, 1, 2, 3\}$  for this example.

**Example 7.5** (Spherical obstacle). We consider the example from [46, Section 4.8.4]. Accordingly, we set  $\Omega$  to be the circle centered at  $(0, 0)$  of radius 1,  $\bar{u} = \infty$ ,  $A$  to be the identity,

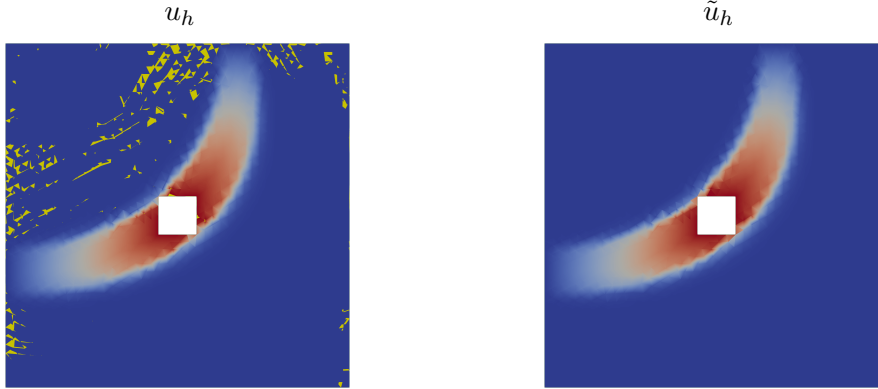


FIGURE 4. (Post processing the solution  $u_h$  to Example 7.3). We set  $p = 2$  and  $h \approx 0.03$ ,  $\epsilon_1 = 0.0$  and  $\epsilon_2 = 0.01$ . Left: Computed solution  $u_h$  that has bound preserving local averages. Right: Limited solution  $\tilde{u}_h$  that is bound preserving.

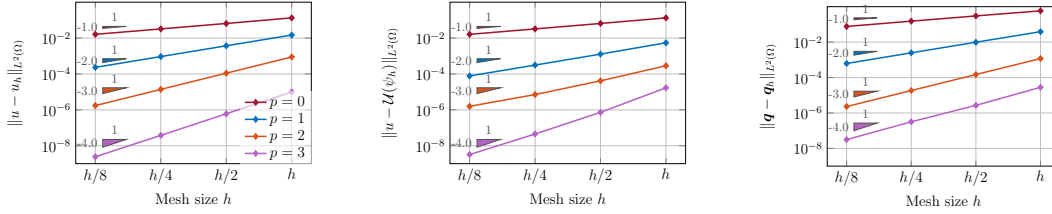


FIGURE 5. (Example 7.4). Computed  $L^2$  errors and rates of the approximations  $(u_h, \mathcal{U}(\psi_h), \mathbf{q}_h)$  of Algorithm 3 with  $\mathcal{U}(\psi_h) = \exp(\psi_h)$ . The algorithm is terminated when  $\|u_h^k - u_h^{k-1}\|_{L^2(\Omega)} < 10^{-12}$  and the tolerance for the Newton solver is set to  $10^{-10}$ . The coarsest mesh size  $h \approx 0.33$ . We set  $\epsilon_1 = 0$  in (155) for all  $p$ . For  $p = 0$  and  $p = 1$ , we set  $\epsilon_2 = 0$ . For  $p = 2$ , we set  $\epsilon_2 = 1e - 05$  and for  $p = 3$ , we set  $\epsilon_2 = 1e - 07$ . In this example, we set  $\alpha^k = 1.5^k$ .

$g = f = 0$ , and

$$\underline{u} = \begin{cases} \sqrt{1/4 - r^2} & \text{if } r \leq 9/20, \\ \varphi(r) & \text{otherwise,} \end{cases} \quad \text{where } r = \sqrt{x^2 + y^2}.$$

In the above,  $\varphi(r)$  is the unique  $C^1$  linear extension of  $r \mapsto \sqrt{1/4 - r^2}$  for  $r > 9/20$ . The exact solution,

$$u = \begin{cases} Q \ln \sqrt{x^2 + y^2} & \text{if } \sqrt{x^2 + y^2} > a, \\ \underline{u} & \text{otherwise,} \end{cases}$$



FIGURE 6. Left: Computed solution  $u_h$  for  $p = 2$  and  $h \approx 0.015$  with  $\epsilon_1 = 0$  and  $\epsilon_2 = 1e - 04$  and  $\mathcal{U}(\psi) = \underline{u} + \exp(\psi)$ . Right: Local mass conservation indicator  $\xi_h$ , plotted with log scale. Observe that we obtain local mass conservation with almost double precision accuracy on elements not intersecting the obstacle.

where  $a = \exp(W_{-1}(-1/(2e^2))/2 + 1) \approx 0.34898$  where  $W_{-1}(\cdot)$  is the  $-1$ -branch of the Lambert W-function, and  $Q = \sqrt{1/4 - a^2}/\ln a$ , belongs to  $H^{5/2-\epsilon}(\Omega)$ . Hence, one can only expect at most an order of  $5/2$  (resp.  $3/2$ ) for  $\|u - u_h\|_{L^2(\Omega)}$  (resp.  $\|\mathbf{q} - \mathbf{q}_h\|_{L^2(\Omega)}$ ).

Figure 6 shows the solution computed with  $p = 2$  along with a local mass conservation indicator  $\xi_h \in V_h^0$  defined as  $\xi_h|_T = |(\nabla \cdot \mathbf{q}_h, 1)_T|$  for all  $T \in \mathcal{T}_h$ . This demonstrates the result stated in Corollary 1; i.e., that the computed solution is locally mass conservative away from the contact zone. Figure 7 reports the rates of decay of the discretization error. For  $p = 2$ , the optimal rate of 1.5 is observed for the flux. For error in the primal variable, we observe a rate of 2.0 for  $p = 1$  and  $p = 2$ .

We now investigate the number of linear solves required per proximal iteration  $k$  for different stopping criteria for Newton’s method. Here, we choose  $\alpha^k = 1$ ,  $p = 1$ , and  $\mathcal{U}(\psi) = \underline{u} + \exp(\psi)$ . We use a quadrature rule with the element vertices and we set  $\epsilon_1 = \epsilon_2 = 0$  in (155). The algorithm is stopped when  $\|u_h^k - u_h^{k-1}\|_{L^2(\Omega)} < 10^{-6}$ .

In Table 2, we use only one linear solve per proximal step and see that the required number of subproblems does not change as the mesh is refined. However, the approximation  $\mathcal{U}(\psi_h)$  stops converging for the last mesh refinement in this case. Decreasing the tolerance on the successive difference of iterates to  $\|u_h^k - u_h^{k-1}\|_{L^2(\Omega)} < 10^{-8}$  fixes this issue but requires more proximal steps. In Table 3 and Table 4, we allow for multiple linear solves per nonlinear problem, stopping Newton’s method when the square root of the inner product between the residual and the linear update reaches a certain tolerance [59]. In Table 3, we set this tolerance to  $10^{-10}$  and observe that the number of linear solves does not change with mesh refinement, and  $\mathcal{U}(\psi_h)$  converges with  $h$ . Finally, in Table 4, we adaptively update the tolerance for Newton’s method based on the successive difference between the two proximal iterates; i.e, we set the Newton tolerance to be  $\min(0.1, \|u_h^k - u_h^{k-1}\|)$ . Here, fewer linear solvers are needed, and  $\mathcal{U}(\psi_h)$  still converges with  $h$ . This leads us to conclude that future research is required to optimize the nonlinear solvers used in proximal Galerkin methods.

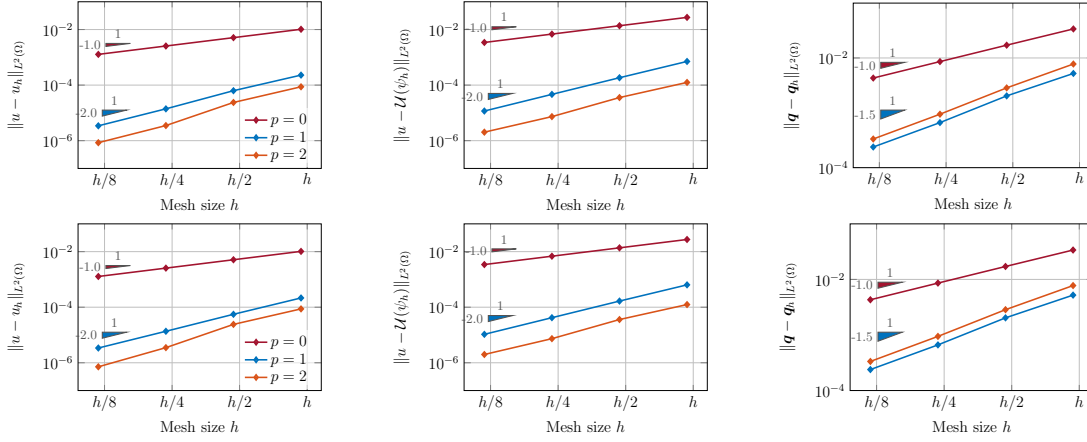


FIGURE 7. (Example 7.5). Computed  $L^2$  errors and rates of the approximations  $(u_h, \mathcal{U}(\psi_h), \mathbf{q}_h)$  of Algorithm 3 with different choices for  $\mathcal{U}$ . (Top row:  $\mathcal{U}(\psi) = \underline{u} + \exp(\psi)$ . Bottom row:  $\mathcal{U}(\psi) = \underline{u} + \ln(1 + \exp(\psi))$ .) The algorithm is terminated once  $\|u_h^k - u_h^{k-1}\|_{L^2(\Omega)} < 10^{-6}$  and the tolerance for the Newton solver is set to  $10^{-10}$ . The coarsest mesh size  $h \approx 0.058$ . For  $p = 0$  and  $p = 1$ , we set  $\epsilon_1 = \epsilon_2 = 0$ . For  $p = 2$ , we set  $\epsilon_1 = 0, \epsilon_2 = 2e - 04$ . In this example, we set  $\alpha^k = 1$ .

$\ A^{-1/2}(\mathbf{q} - \mathbf{q}_h^k)\ _{L^2(\Omega)}$					
$k$	Linear solves	$h$	$h/2$	$h/4$	$h/8$
1	1	5.163e-01	5.163e-01	5.163e-01	5.163e-01
2	1	4.543e-01	4.543e-01	4.543e-01	4.543e-01
3	1	2.567e-01	2.567e-01	2.568e-01	2.568e-01
$\vdots$	$\vdots$	$\vdots$	$\vdots$	$\vdots$	$\vdots$
Total iterations $k$		14	13	13	13
Total linear solves		14	13	13	13
Final error: $\ A^{-1/2}(\mathbf{q} - \mathbf{q}_h^k)\ _{L^2(\Omega)}$		5.240e-03	2.054e-03	6.852e-04	2.774e-04
Final error: $\ u - \mathcal{U}(\psi_h^k)\ _{L^2(\Omega)}$		7.114e-04	1.847e-04	4.660e-05	3.062e-03

TABLE 2. (One Newton step per proximal step). Number of linear solves needed per proximal Galerkin iteration  $k$  and the corresponding error  $\|A^{-1/2}(\mathbf{q} - \mathbf{q}_h^k)\|_{L^2(\Omega)}$ .

## REFERENCES

- [1] Ivar Aavatsmark, Tor Barkve, Oistein Bøe, and Trond Mannseth. Discretization on unstructured grids for inhomogeneous, anisotropic media. Part I: Derivation of the methods. *SIAM Journal on Scientific Computing*, 19(5):1700–1716, 1998.
- [2] Tristan Pryer Abdolreza Amiri, Gabriel R. Barrenechea. A nodally bound-preserving finite element method for reaction-convection-diffusion equations. *arXiv preprint arXiv:2311.15602 [math.NA]*, 2023.
- [3] Lukáš Adam, Michael Hintermüller, and Thomas Michael Surowiec. A semismooth Newton method with analytical path-following for the-projection onto the Gibbs simplex. *IMA Journal of Numerical Analysis*, 39(3):1276–1295, 2019.
- [4] Antonio Ambrosetti and Giovanni Prodi. *A Primer of Nonlinear Analysis*. Cambridge University Press, 1995.

$\ A^{-1/2}(\mathbf{q} - \mathbf{q}_h^k)\ _{L^2(\Omega)}$					
$k$	Linear solves	$h$	$h/2$	$h/4$	$h/8$
1	7	3.408e-01	3.408e-01	3.408e-01	3.408e-01
2	6-7	8.277e-02	8.272e-02	8.271e-02	8.271e-02
3	7	2.298e-02	2.247e-02	2.242e-02	2.242e-02
$\vdots$	$\vdots$	$\vdots$	$\vdots$	$\vdots$	$\vdots$
Total iterations $k$		12	12	12	11
Total linear solves		59	62	63	63
Final error: $\ A^{-1/2}(\mathbf{q} - \mathbf{q}_h^k)\ _{L^2(\Omega)}$		5.219e-03	2.034e-03	6.633e-04	2.381e-04
Final error: $\ u - \mathcal{U}(\psi_h^k)\ _{L^2(\Omega)}$		7.104e-04	1.842e-04	4.640e-05	1.166e-05

TABLE 3. (Newton tolerance =  $10^{-10}$ ). Number of linear solves needed per proximal Galerkin iteration  $k$  and the corresponding error  $\|A^{-1/2}(\mathbf{q} - \mathbf{q}_h^k)\|_{L^2(\Omega)}$ .

$\ A^{-1/2}(\mathbf{q} - \mathbf{q}_h^k)\ _{L^2(\Omega)}$					
$k$	Linear solves	$h$	$h/2$	$h/4$	$h/8$
1	3	3.389e-01	3.389e-01	3.389e-01	3.389e-01
2	3	8.059e-02	8.055e-02	8.054e-02	8.054e-02
3	3	2.265e-02	2.213e-02	2.208e-02	2.208e-02
$\vdots$	$\vdots$	$\vdots$	$\vdots$	$\vdots$	$\vdots$
Total iterations $k$		12	12	12	11
Total linear solves		27	27	28	27
Final error: $\ A^{-1/2}(\mathbf{q} - \mathbf{q}_h^k)\ _{L^2(\Omega)}$		5.219e-03	2.034e-03	6.633e-04	2.381e-04
Final error: $\ u - \mathcal{U}(\psi_h^k)\ _{L^2(\Omega)}$		7.104e-04	1.842e-04	4.641e-05	1.166e-05

TABLE 4. (Newton tolerance =  $\min(0.1, \|u_h^k - u_h^{k-1}\|_{L^2(\Omega)})$ ). Number of linear solves needed per proximal Galerkin iteration  $k$  and the corresponding error  $\|A^{-1/2}(\mathbf{q} - \mathbf{q}_h^k)\|_{L^2(\Omega)}$ .

- [5] Jürgen Appell and Petr P. Zabrejko. *Nonlinear Superposition Operators*. Cambridge Tracts in Mathematics. Cambridge University Press, 1990.
- [6] D. N. Arnold and F. Brezzi. Mixed and nonconforming finite element methods: implementation, postprocessing and error estimates. *RAIRO Modél. Math. Anal. Numér.*, 19(1):7–32, 1985.
- [7] Douglas N Arnold and Franco Brezzi. Mixed and nonconforming finite element methods: implementation, postprocessing and error estimates. *ESAIM: Mathematical Modelling and Numerical Analysis*, 19(1):7–32, 1985.
- [8] Gabriel R Barrenechea, Emmanuil H Georgoulis, Tristan Pryer, and Andreas Veiser. A nodally bound-preserving finite element method. *IMA Journal of Numerical Analysis*, 44(4):2198–2219, 2024.
- [9] Gabriel R Barrenechea, Volker John, and Petr Knobloch. Finite element methods respecting the discrete maximum principle for convection-diffusion equations. *SIAM Review*, 66(1):3–88, 2024.
- [10] Gabriel R. Barrenechea, Volker John, Petr Knobloch, and Richard Rankin. A unified analysis of algebraic flux correction schemes for convection-diffusion equations. *SeMA J.*, 75(4):655–685, 2018.
- [11] Heinz H Bauschke, Jonathan M Borwein, et al. Legendre functions and the method of random Bregman projections. *Journal of Convex Analysis*, 4(1):27–67, 1997.
- [12] HH Bauschke. *Convex Analysis and Monotone Operator Theory in Hilbert Spaces*, 2011.
- [13] Daniele Boffi, Franco Brezzi, and Michel Fortin. *Mixed Finite Element Methods and Applications*, volume 44 of *Springer Series in Computational Mathematics*. Springer, Heidelberg, 2013.

- [14] L.M. Bregman. The relaxation method of finding the common point of convex sets and its application to the solution of problems in convex programming. *USSR Computational Mathematics and Mathematical Physics*, 7(3):200–217, 1967.
- [15] Franco Brezzi, William W Hager, and PA Raviart. Error estimates for the finite element solution of variational inequalities: Part II. Mixed methods. *Numerische Mathematik*, 31(1):1–16, 1978.
- [16] Franco Brezzi, William W Hager, and Pierre-Arnaud Raviart. Error estimates for the finite element solution of variational inequalities: Part I. Primal theory. *Numerische Mathematik*, 28(4):431–443, 1977.
- [17] Ed Bueler and Patrick E. Farrell. A full approximation scheme multilevel method for nonlinear variational inequalities. *SIAM Journal on Scientific Computing*, 46(4):A2421–A2444, 2024.
- [18] Erik Burman and Alexandre Ern. Stabilized Galerkin approximation of convection–diffusion–reaction equations: Discrete maximum principle and convergence. *Math. Comp.*, 74(252):1637–1652, 2005.
- [19] Philippe G Ciarlet. *The Finite Element Method for Elliptic Problems*. SIAM, 2002.
- [20] Philippe G Ciarlet. *Linear and Nonlinear Functional Analysis with Applications*, volume 130. SIAM, 2013.
- [21] Philippe G Ciarlet and P-A Raviart. Maximum principle and uniform convergence for the finite element method. *Computer methods in applied mechanics and engineering*, 2(1):17–31, 1973.
- [22] Bernardo Cockburn, Guosheng Fu, and Weifeng Qiu. Discrete  $H^1$ -inequalities for spaces admitting M-decompositions. *SIAM J. Numer. Anal.*, 56(6):3407–3429, 2018.
- [23] Jørgen S Dokken, Patrick E Farrell, Brendan Keith, and Thomas M Surowiec. The latent variable proximal point algorithm for variational problems with pointwise constraints. *In preparation*, 2025.
- [24] Herbert Egger and Joachim Schöberl. A hybrid mixed discontinuous Galerkin finite-element method for convection–diffusion problems. *IMA Journal of Numerical Analysis*, 30(4):1206–1234, 2010.
- [25] A. Ern and J. L. Guermond. *Finite Elements I*. Texts in Applied Mathematics. Springer International Publishing, 2021.
- [26] Alexandre Ern, Thirupathi Gudi, Iain Smears, and Martin Vohralík. Equivalence of local-and global-best approximations, a simple stable local commuting projector, and optimal hp approximation estimates in  $H(\operatorname{div})$ . *IMA Journal of Numerical Analysis*, 42(2):1023–1049, 2022.
- [27] Alexandre Ern and Jean-Luc Guermond. Finite element quasi-interpolation and best approximation. *ESAIM: Mathematical Modelling and Numerical Analysis*, 51(4):1367–1385, 2017.
- [28] Alexandre Ern and Jean-Luc Guermond. *Finite elements II*. Springer, 2021.
- [29] Alexandre Ern and Jean-Luc Guermond. Quasi-optimal nonconforming approximation of elliptic PDEs with contrasted coefficients and  $H^{1+r}$ ,  $r > 0$ , regularity. *Foundations of Computational Mathematics*, 22:1273–1308, 2021.
- [30] Patrick E Farrell, Matteo Croci, and Thomas M Surowiec. Deflation for semismooth equations. *Optimization Methods and Software*, 35(6):1248–1271, 2020.
- [31] Michel Fortin and Franco Brezzi. *Mixed and Hybrid Finite Element Methods*, volume 51. New York: Springer-Verlag, 1991.
- [32] Huadong Gao and Weifeng Qiu. Error analysis of mixed finite element methods for nonlinear parabolic equations. *Journal of Scientific Computing*, 77(3):1660–1678, 2018.
- [33] Roland Glowinski and Patrick Le Tallec. *Augmented Lagrangian and operator-splitting methods in nonlinear mechanics*. SIAM, 1989.
- [34] Carsten Gräser and Ralf Kornhuber. Multigrid methods for obstacle problems. *Journal of Computational Mathematics*, pages 1–44, 2009.
- [35] David Green, Xiaozhe Hu, Jeremy Lore, Lin Mu, and Mark L Stowell. An efficient high-order numerical solver for diffusion equations with strong anisotropy. *Computer Physics Communications*, 276:108333, 2022.
- [36] David Green, Xiaozhe Hu, Jeremy Lore, Lin Mu, and Mark L Stowell. An efficient high-order solver for diffusion equations with strong anisotropy on non-anisotropy-aligned meshes. *SIAM Journal on Scientific Computing*, 46(2):S199–S222, 2024.
- [37] Ralf Greve and Heinz Blatter. *Dynamics of ice sheets and glaciers*. Springer Science & Business Media, 2009.
- [38] Tom Gustafsson, Rolf Stenberg, and Juha Videman. Mixed and stabilized finite element methods for the obstacle problem. *SIAM Journal on Numerical Analysis*, 55(6):2718–2744, 2017.
- [39] Tom Gustafsson, Rolf Stenberg, and Juha Videman. On finite element formulations for the obstacle problem–mixed and stabilised methods. *Computational Methods in Applied Mathematics*, 17(3):413–429, 2017.

- [40] Raphaële Herbin and Florence Hubert. Benchmark on discretization schemes for anisotropic diffusion problems on general grids (December 10th).
- [41] Michael Hintermüller, Kazufumi Ito, and Karl Kunisch. The primal-dual active set strategy as a semismooth Newton method. *SIAM Journal on Optimization*, 13(3):865–888, 2002.
- [42] Michael Hintermüller and Karl Kunisch. Feasible and noninterior path-following in constrained minimization with low multiplier regularity. *SIAM Journal on Control and Optimization*, 45(4):1198–1221, 2006.
- [43] Michael Hintermüller and Karl Kunisch. Path-following methods for a class of constrained minimization problems in function space. *SIAM Journal on Optimization*, 17(1):159–187, 2006.
- [44] Tommi Kärkkäinen, Karl Kunisch, and Pasi Tarvainen. Augmented lagrangian active set methods for obstacle problems. *Journal of optimization theory and applications*, 119:499–533, 2003.
- [45] Brendan Keith, Dohyun Kim, Boyan S Lazarov, and Thomas M Surowiec. Analysis of the SiMPL method for density-based topology optimization. *arXiv preprint arXiv:2409.19341*, 2024.
- [46] Brendan Keith and Thomas M Surowiec. Proximal galerkin: A structure-preserving finite element method for pointwise bound constraints. *Foundations of Computational Mathematics*, pages 1–97, 2024.
- [47] Dohyun Kim, Boyan Stefanov Lazarov, Thomas M. Surowiec, and Brendan Keith. A simple introduction to the SiMPL method for density-based topology optimization, 2024.
- [48] David Kinderlehrer and Guido Stampacchia. *An introduction to variational inequalities and their applications*. SIAM, 2000.
- [49] Robert C Kirby and Daniel Shapero. High-order bounds-satisfying approximation of partial differential equations via finite element variational inequalities. *Numerische Mathematik*, pages 1–21, 2024.
- [50] Keegan L A Kirk, Beatrice Riviere, and Rami Masri. Numerical analysis of a hybridized discontinuous Galerkin method for the Cahn–Hilliard problem. *IMA Journal of Numerical Analysis*, 44(5):2752–2792, 11 2023.
- [51] Andris Lasis and Endre Süli. hp-version discontinuous Galerkin finite element method for semilinear parabolic problems. *SIAM Journal on Numerical Analysis*, 45(4):1544–1569, 2007.
- [52] Xianping Li and Weizhang Huang. An anisotropic mesh adaptation method for the finite element solution of heterogeneous anisotropic diffusion problems. *Journal of Computational Physics*, 229(21):8072–8094, 2010.
- [53] JL Lions. Quelques methodes de resolution des problemes aux limites non lineaires. *Dunford/Gauthier-Villars*, 1969.
- [54] Ioannis P. A. Papadopoulos. Hierarchical proximal Galerkin: a fast *hp*-FEM solver for variational problems with pointwise inequality constraints, 2024.
- [55] Ioannis PA Papadopoulos, Patrick E Farrell, and Thomas M Surowiec. Computing multiple solutions of topology optimization problems. *SIAM Journal on Scientific Computing*, 43(3):A1555–A1582, 2021.
- [56] P. A. Raviart and J. M. Thomas. A mixed finite element method for 2-nd order elliptic problems. In Ilio Galligani and Enrico Magenes, editors, *Mathematical Aspects of Finite Element Methods*, pages 292–315, Berlin, Heidelberg, 1977. Springer Berlin Heidelberg.
- [57] R. Tyrrell Rockafellar. Monotone operators and the proximal point algorithm. *SIAM Journal on Control and Optimization*, 14(5):877–898, 1976.
- [58] J-F Rodrigues. *Obstacle problems in mathematical physics*. Elsevier, 1987.
- [59] Joachim Schöberl. C++ 11 implementation of finite elements in ngsolve. *Institute for Analysis and Scientific Computing, Vienna University of Technology*, 30, 2014.
- [60] Reinhard Scholz. Numerical solution of the obstacle problem by the penalty method. *Computing (Wien. Print)*, 32(4):297–306, 1984.
- [61] Marc Teboulle. A simplified view of first order methods for optimization. *Mathematical Programming*, 170(1):67–96, 2018.
- [62] Barbara Wohlmuth. Variationally consistent discretization schemes and numerical algorithms for contact problems. *Acta Numerica*, 20:569–734, 2011.
- [63] Jinchao Xu and Ludmil Zikatanov. A monotone finite element scheme for convection-diffusion equations. *Mathematics of Computation*, 68(228):1429–1446, 1999.
- [64] Xiangxiong Zhang and Chi-Wang Shu. On maximum-principle-satisfying high order schemes for scalar conservation laws. *Journal of Computational Physics*, 229(9):3091–3120, 2010.

## APPENDIX A. PROOF OF LEMMA 4.4

*Proof.* First, observe that

$$(156) \quad \mathcal{A}_h((\mathbf{q}_h, u_h, \hat{u}_h), (\mathbf{q}_h, u_h, \hat{u}_h)) = \|A^{-1/2}\mathbf{q}_h\|_{L^2(\Omega)}^2$$

From [24, Lemma 3.1], see also [32, lemma 3.1] for a detailed proof, there exists  $\boldsymbol{\tau}_h \in \boldsymbol{\Sigma}_h^p$  such that for any  $T \in \mathcal{T}_h$  and for all  $\mathbf{p} \in \mathbb{P}^{p-1}(T)^d$  and  $q \in \mathbb{P}^p(\partial T)$ ,

$$(157) \quad (\boldsymbol{\tau}_h, \mathbf{p})_T + \langle \boldsymbol{\tau}_h \cdot \mathbf{n}, q \rangle_{\partial T} = (A^{-1}\nabla_h u_h, \mathbf{p})_T + \langle h_T^{-1}(\hat{u}_h - u_h), q \rangle_{\partial T},$$

and

$$(158) \quad \|\boldsymbol{\tau}_h\|_{\mathcal{T}_h}^2 \leq c_I(\|A^{-1}\nabla_h u_h\|_{\mathcal{T}_h}^2 + \|h_T^{-1/2}(u_h - \hat{u}_h)\|_{\partial\mathcal{T}_h}^2).$$

Then, for  $\gamma > 0$ , we have that

$$(159) \quad \mathcal{B}_h(\gamma\boldsymbol{\tau}_h, (u_h, \hat{u}_h)) = \gamma(\|A^{-1/2}\nabla_h u_h\|_{\mathcal{T}_h}^2 + \|h_T^{-1/2}(u_h - \hat{u}_h)\|_{\partial\mathcal{T}_h}^2)$$

It then follows that

$$(160) \quad \begin{aligned} \mathcal{A}_h((\mathbf{q}_h, u_h, \hat{u}_h), (\gamma\boldsymbol{\tau}_h, 0, 0)) - (A^{-1}\mathbf{q}_h, \gamma\boldsymbol{\tau}_h) \\ = \gamma(\|A^{-1/2}\nabla_h u_h\|_{\mathcal{T}_h}^2 + \|h_T^{-1/2}(u_h - \hat{u}_h)\|_{\partial\mathcal{T}_h}^2). \end{aligned}$$

Using Cauchy-Schwarz and Young's inequalities, we obtain that

$$\begin{aligned} |(A^{-1}\mathbf{q}_h, \gamma\boldsymbol{\tau}_h)| &\leq \gamma\|A^{-1/2}\|_{L^\infty(\Omega)}\|A^{-1/2}\mathbf{q}_h\|_{\mathcal{T}_h}\|\boldsymbol{\tau}_h\|_{\mathcal{T}_h} \\ &\leq \frac{1}{2}\|A^{-1/2}\mathbf{q}_h\|_{\mathcal{T}_h}^2 + \frac{\gamma^2 c_{ICA}}{2}(\|A^{-1/2}\nabla_h u_h\|_{\mathcal{T}_h}^2 + \|h_T^{-1/2}(u_h - \hat{u}_h)\|_{\partial\mathcal{T}_h}^2) \end{aligned}$$

Thus, choosing  $\gamma = 1/(c_{ICA})$  and adding (156) with (160) yield

$$(161) \quad \mathcal{A}_h((\mathbf{q}_h, u_h, \hat{u}_h), (\gamma\boldsymbol{\tau}_h + \mathbf{q}_h, u_h, \hat{u}_h)) \gtrsim \|(\mathbf{q}_h, u_h, \hat{u}_h)\|^2.$$

The proof of (58) follows from applications of discrete trace inequalities, see [24, Proposition 3.4]. We omit the details.  $\square$

## APPENDIX B. PROOF OF COROLLARY 2

*Proof.* (Corollary 2) Select  $\mathbf{r}_h = \mathbf{\Pi}_h \boldsymbol{\sigma}(u)$  where  $\mathbf{\Pi}_h$  is the local  $L^2$ -projection onto the space  $\mathbb{P}^0(T)^d$ . Note that  $\mathbf{r}_h \in \boldsymbol{\Sigma}_h^p$  and  $\nabla \cdot \mathbf{r}_h = 0$ . By definition of the norm  $\|\cdot\|_{\mathcal{S}^d}$  (122) and stability of the  $L^2$ -projection (averaging operator) in  $L^\rho(T)$ , we obtain that

$$(162) \quad \begin{aligned} \|\boldsymbol{\sigma}(u) - \mathbf{r}_h\|_{\mathcal{S}^d} &\leq h^s \|A^{-1/2}(\boldsymbol{\sigma}(u) - \mathbf{r}_h)\|_{L^\rho(\Omega)} + h \|A^{-1/2}\nabla \cdot \boldsymbol{\sigma}(u)\|_{L^2(\Omega)} \\ &\lesssim h^s (|u|_{H^{1+s}(\Omega)} + h^{1-s} \|\nabla \cdot (\boldsymbol{\sigma}(u))\|_{L^2(\Omega)}). \end{aligned}$$

In the above, we also used the embedding  $H^s(\Omega)^d \hookrightarrow L^\rho(\Omega)^d$ . Further, according to [27, Lemma 7.1], we also have a Poincaré inequality in  $H^s(T)$ :

$$(163) \quad \|\boldsymbol{\sigma}(u) - \mathbf{r}_h\|_{L^2(T)} \lesssim h_T^s |\boldsymbol{\sigma}(u)|_{H^s(T)} \lesssim h_T^s \|u\|_{H^{1+s}(T)}.$$

For  $v_h$ , select  $v_h = \mathcal{I}_h u$  a quasi-interpolant of  $u$  [27, Section 6] which satisfies

$$(164) \quad \|u - \mathcal{I}_h u\|_{L^2(T)} + h \|\nabla(u - \mathcal{I}_h u)\|_{L^2(T)} \lesssim h^{1+s} |u|_{H^{1+s}(\Delta_T)},$$



where  $\Delta_T$  is a macro-element. We may also select  $\hat{v}_h = \mathcal{I}_h u \in M_{h,0}^p$  since it is single valued on interior facets and  $\mathcal{I}_h u|_{\partial\Omega} = 0$ . This implies that the third term in  $\|(\boldsymbol{\sigma}(u) - \boldsymbol{r}_h, u - v_h, u - \hat{v}_h)\|$  is zero. Collecting the above observations and summing over elements yield

$$(165) \quad \mathcal{E}(u) \lesssim h^s(|u|_{H^{1+s}(\Omega)} + h^{1-s}\|\nabla \cdot (\boldsymbol{\sigma}(u))\|_{L^2(\Omega)}).$$

Proceeding, we bound  $\mathcal{E}(\delta)$ . Selecting  $\varphi_h = \Pi_h \delta$ , the  $L^2$ - projection onto  $V_h^p$ , we derive

$$(166) \quad \|\delta - \Pi_h \delta\|_{H^1(\mathcal{T}_h)^*} = \sup_{w \in H^1(\mathcal{T}_h)} \frac{(\delta - \Pi_h \delta, w - \Pi_h w)}{\|w\|_{\text{DG}}}$$

With the approximation properties of the  $L^2$  projection, we estimate

$$(167) \quad \|w - \Pi_h w\|_{L^2(\Omega)} \leq h \|\nabla_h w\|_{\mathcal{T}_h}.$$

From the  $L^2$  stability of  $\Pi_h$ , it follows that

$$\|\delta - \Pi_h \delta\|_{H^1(\mathcal{T}_h)^*} \lesssim h \|\delta\|_{L^2(\Omega)}.$$

The second term in  $\mathcal{E}(\delta)$  is bounded by approximation properties of the  $L^2$ -projection.  $\square$